GAS LASER POWER SUPPLIES

The power supplies for continuous-wave gas lasers are similar in design to those used in direct-current power supplies. Gas laser power supplies tend to be current-limited regulated DC power supplies. The designs are basically the same for all gas-discharge devices. The details depend on the particular voltage-current characteristics of the gas and the configuration of the laser. Three essential elements are used in the design of all gas laser power supplies: the starter or ignition circuit, the operating supply, and a current-limiting element.

Electrical Characteristics of Gas Discharges

Most gas lasers are pumped by an electrical discharge that flows through the gas mixture between electrodes in the gas. Collisions between electrons in the electric discharge and the molecules in the gas transfer energy from the electrons to the energy levels of the molecule. Electrical discharges in gases are characterized by current/voltage characteristics shown in Figure 1. The exact characteristics, of course, depend on the nature of the gas, its pressure, and the length and diameter of the discharge.

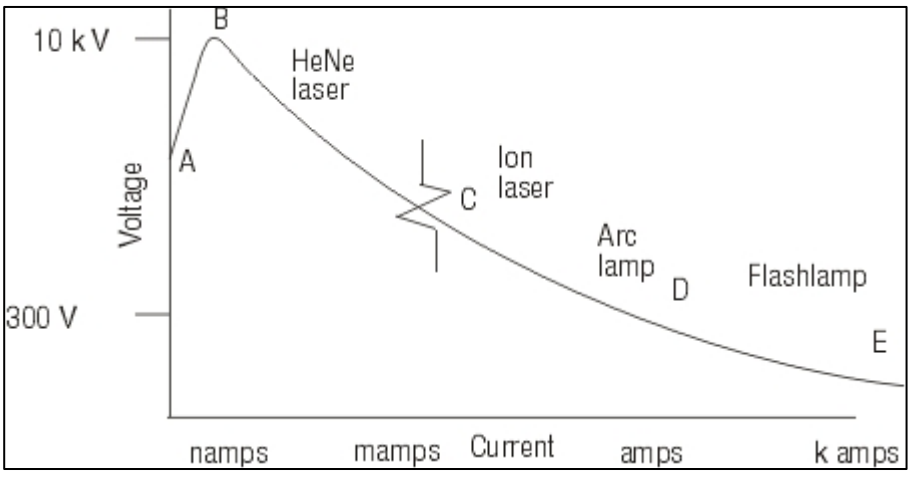

Fig.1Current/voltage curve for a gas discharge curve

The requirements for power supplies for gas lasers derive from the characteristics of the curve in Figure 1. The exact design for a particular gas laser power supply will depend on the specific current/voltage curve for the gas mixture that is being excited, but three essential elements for any gas laser power supply are:

- A starter circuit. This portion of the power supply provides an initial voltage pulse. The peak value of the voltage pulse must exceed the breakdown voltage of the gas. The pulse drives the gas past point B and into region C.

- Operating supply. This part of the power supply provides a steady current flow through the gas mix, after the gas has reached region C. It must operate at the appropriate voltage and current levels to sustain the current in the particular gas.

- Current limiter. This limits the current through the gas to a desired value and prohibits the unbounded increase of current. It usually takes the form of a ballast resistor in series with the discharge.

Power Supplies for Helium-Neon Lasers

In steady operation, the power supply must sustain the flow of electrical current through the gas mixture, accelerating free electrons to energies sufficient for excitation of the helium atoms and providing enough current flow to produce an adequate population inversion.

The basic blocks of the power supply for a typical small helium-neon laser are shown in Figure 2.

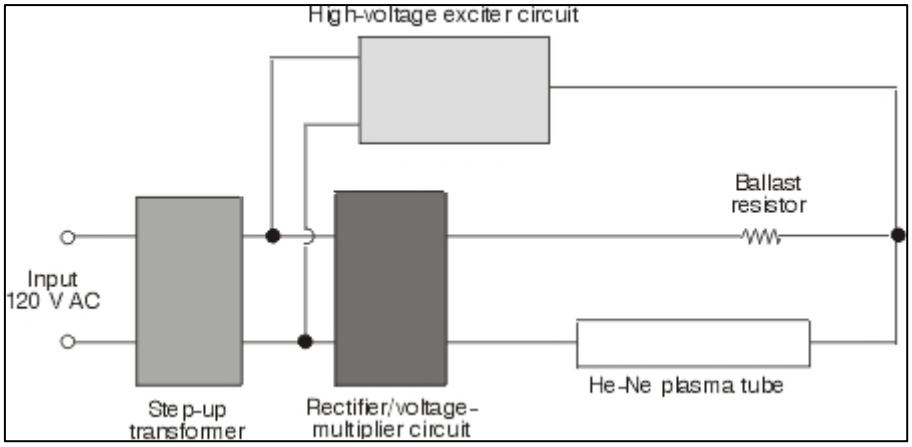

Fig.2 Block diagram of power supply for helium-neon laser

The characteristics of the power supply for the helium-neon laser derive from the properties of the current/voltage curve for the helium-neon gas mixture. We already have discussed the general properties of current/voltage curves with respect to Figure 1.

We now discuss some details of circuits that have been used for driving helium-neon lasers. A number of different configurations have been used by different manufacturers. We shall not attempt to describe them all, but shall choose some representative examples.

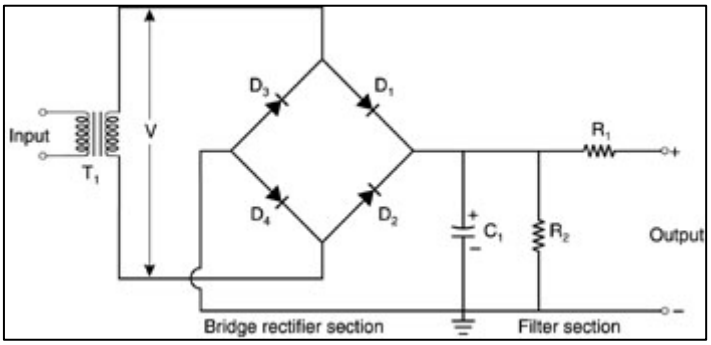

Fig. 3 Full-wave Bridge operating supply.

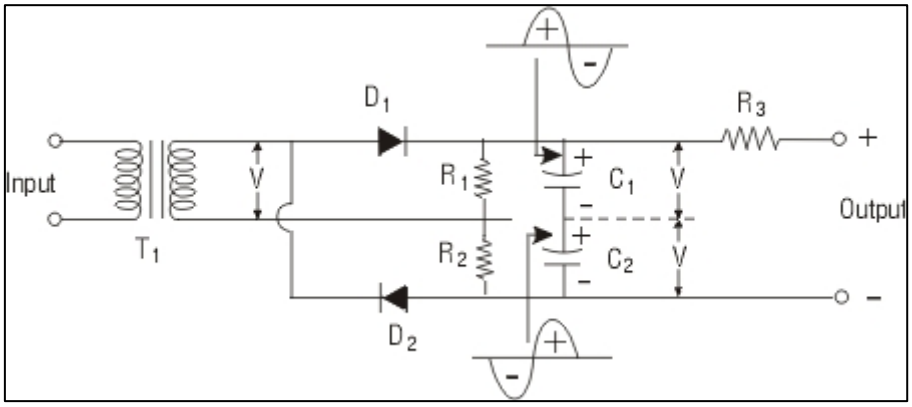

Fig. 4 Operating supply combining rectifier and voltage-doubler functions.

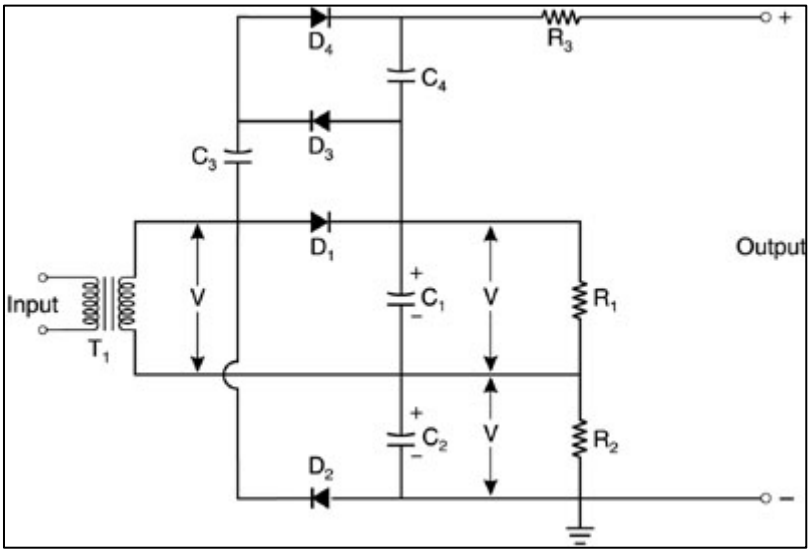

Fig.5 Voltage doubler with internal starting circuit.

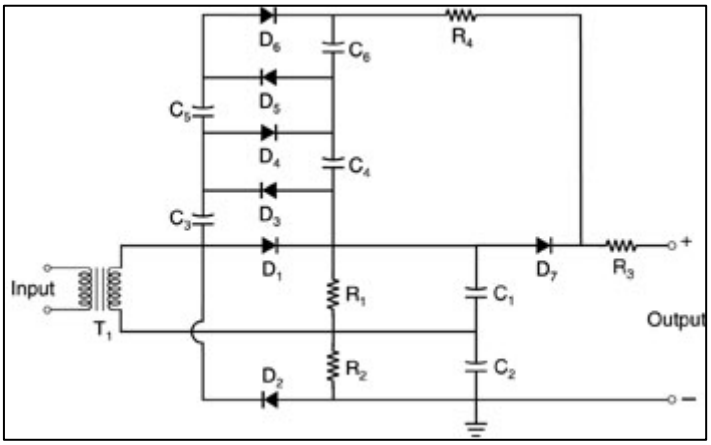

Fig.6 Alternate voltage doubler with internal starting circuit

Figure 7 shows how the output power varies as a function of tube current for a small helium-neon laser. The results are for a laser tube with internal diameter of 1 mm and length 30 cm.

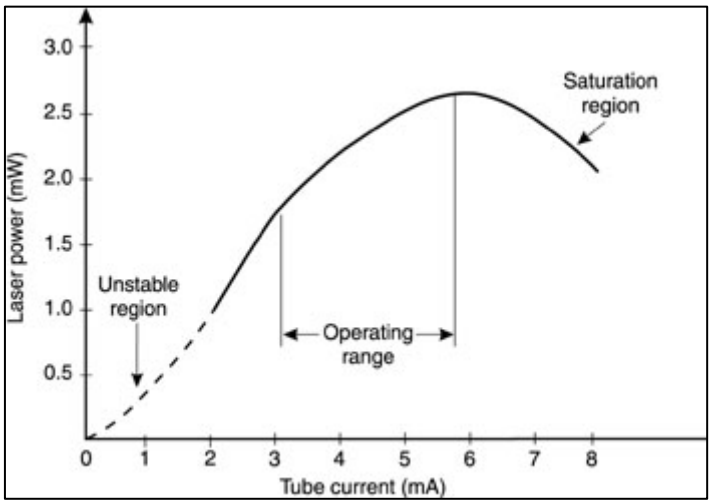

Fig. 7 Power output of helium-neon laser as a function of tube current

Switching Elements

Helium-neon lasers almost always are operated continuously. After the startup, there is no need for high-voltage pulsing of the power supply. We now shall turn to a discussion of gas lasers that frequently are operated as pulsed lasers, and for which there is a need for short-duration high-voltage pulses. As a preliminary to the discussion of these lasers, we first shall describe high-voltage switching elements that often are employed with pulsed gas lasers. The two high-voltage switches that we will describe are spark gaps and thyratrons.

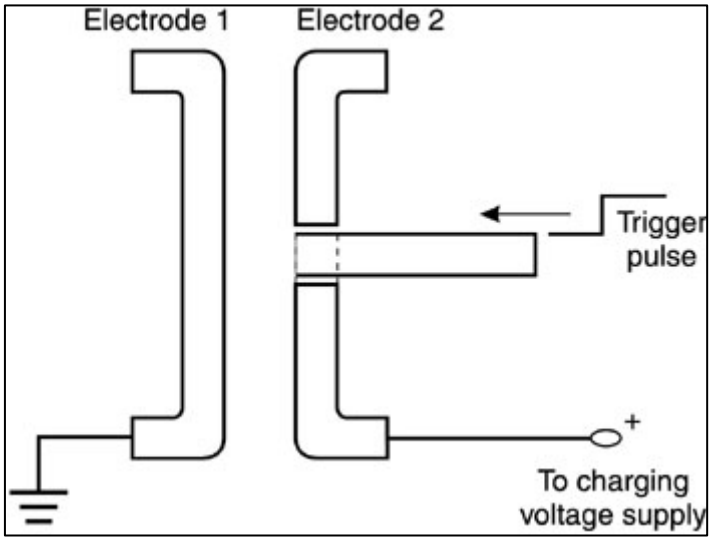

Fig. 8 Diagram of structure of one type of spark gap.
Electrode 2 is in the form of a ring with a hole in the center.

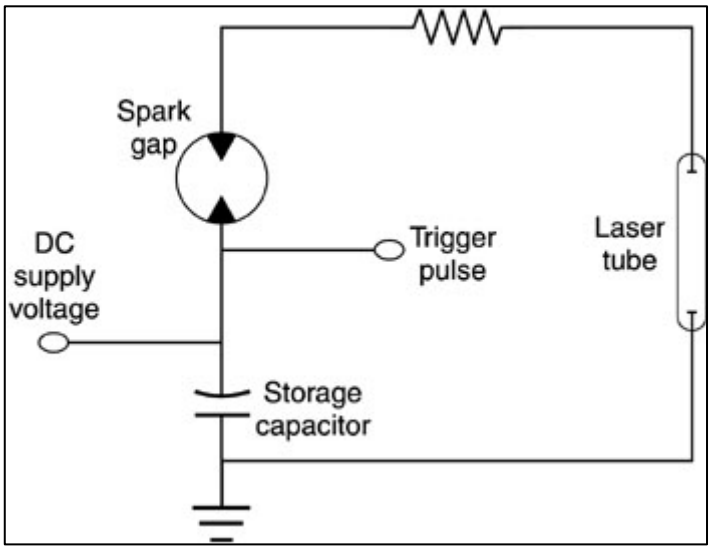

Fig. 9 Trigger circuit using spark gap

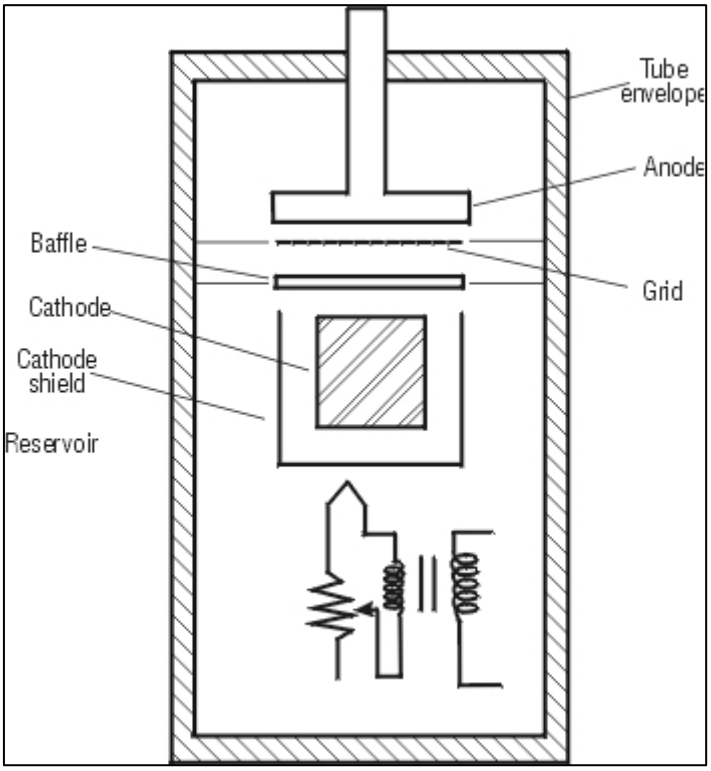

Fig. 10 Schematic drawing of typical thyratron

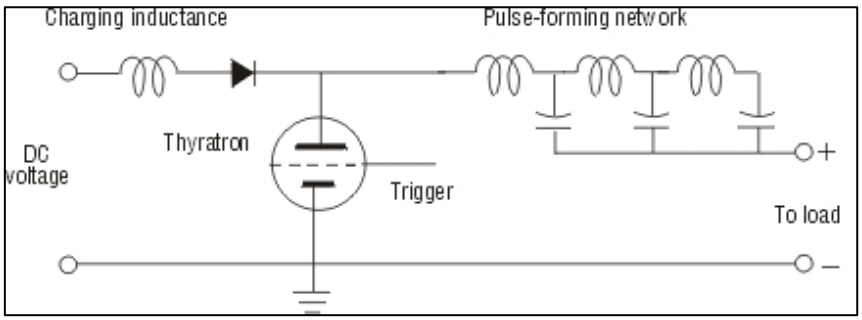

Fig. 11 Pulse circuit using thyratron trigger

Design considerations and scaling laws for CO_2 lasers

The Class I CW CO_2 laser was the first CO_2 laser developed, and continues to be the most common. Figure 1 is a diagram of such a laser. Common characteristics of this CO_2 laser class include the following:

1. Water or oil cooling by use of a double-walled glass plasma tube.

2. Gas flow at a low rate (1-20 liters per minute, depending upon size and output of laser).

3. Dc excitation, coaxial with gas flow and laser beam.

4. Low-current operation (3-100 mA).

5. Gas pressures of 10 to 30 torr.

6. Tube diameters of 1.0-2.0 cm.

7. Available output powers up to about 50 W per meter of tube length.

The primary factor that limits output power of (class I) lasers is their inability to efficiently remove waste heat from the gas. Cooling is principally achieved by helium (He) collisions with tube walls. Air cooling of CO_2 laser tubes is possible, but this results in an elevated wall temperature and greatly reduces laser efficiency. Smaller CO_2 lasers and those used in research often employ water cooling. Industrial CO_2 lasers usually use recirculating oil and oil-to-water heat exchangers for better system stability and reduced maintenance. An increase of tube current beyond the recommended operating value results in more heat than can be effectively removed from the system in this manner. Increases in tube diameter also decrease cooling efficiency by increasing the path length necessary for (He) atoms to reach the walls from the center of the tube. Thus, the only effective method of increasing output power of this type of CO_2 laser is to extend the active length. For best results, this must also be accompanied by an increase in gas flow rate. In larger systems the gas is recirculated with a few percent being replaced on each cycle.

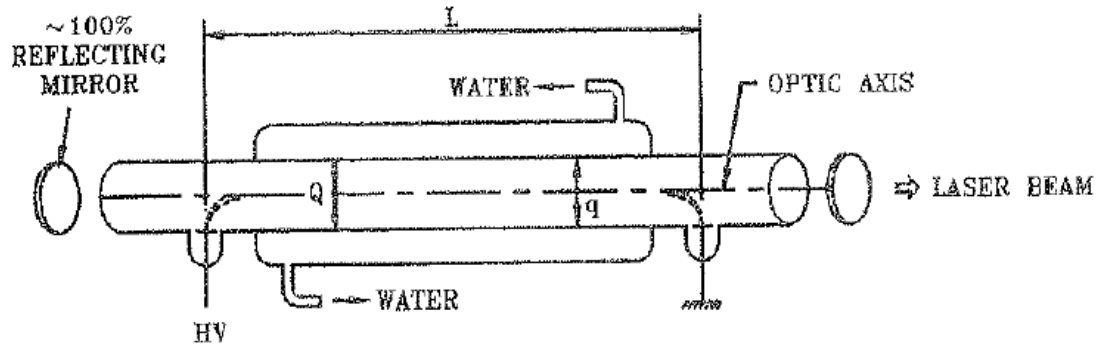

(a) DIFFUSION COOLED LASER

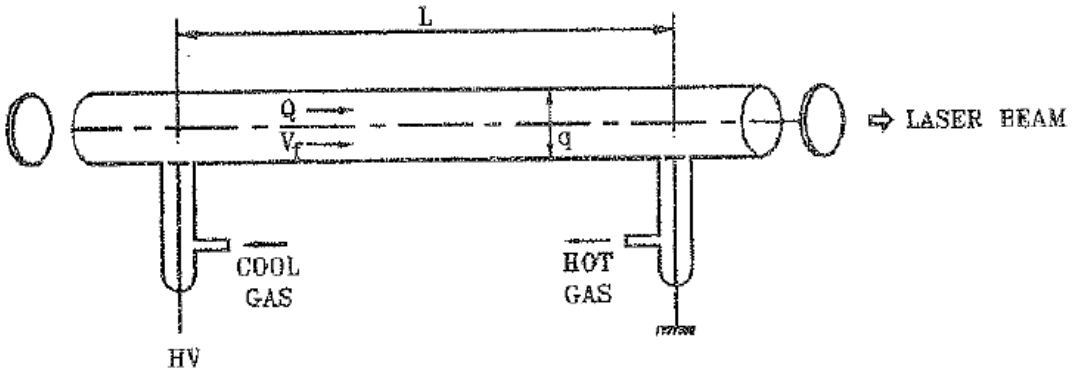

(b) FAST AXIAL FLOW LASER

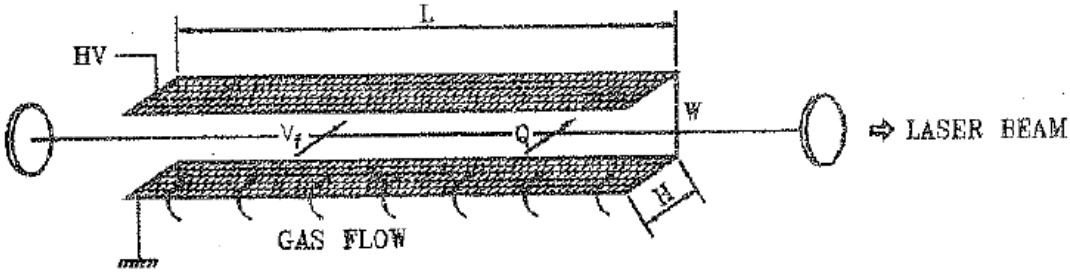

(c) TRANSVERSE FLOW LASER

Figure 1. Schematic diagram of different types of CO_2 laser. Q: Heat flux, q: charged particle flux, V_f: gas flow velocity.

Laser power scaling in various types CO_2 lasers

The output power of a laser scales up with the input power. In a CO_2 laser, the input electrical power density is limited by two factors: first is the rise in laser gas temperature, optimum being, $\Delta T_{opt} = 200$–$250°C$. This limits the input power density P_{in} as the following:

$$P_{in} \leq (1-\eta)^{-1} \cdot \rho \cdot C_p \cdot \Delta T_{opt}/t_c = P_c \quad \text{(say)}, \tag{1}$$

where ρ and C_p are the density and the specific heat of the laser gas respectively, η is the electro-optic efficiency and t_c is the gas cooling time.

Second limiting factor for the input electrical power is the discharge instability, the most common being the ionization thermal instability. In order to avoid the discharge instability, the input power density should be [15]

$$P_{in} \leq 1/A \cdot \rho \cdot C_p \cdot \Delta T/t_s = P_s \quad \text{(say)}, \tag{2}$$

where A is a rate coefficient which is mainly determined by the slope of the dependence of the ionization rate on the discharge parameter E/p, and t_s is the characteristic decay time for any fluctuation in the electron density. The typical value of A is about 10 for the usual laser operating conditions. For efficient and reliable laser operation the input power density should be smaller than the above two limits determined by the cooling and the discharge stabilization processes.

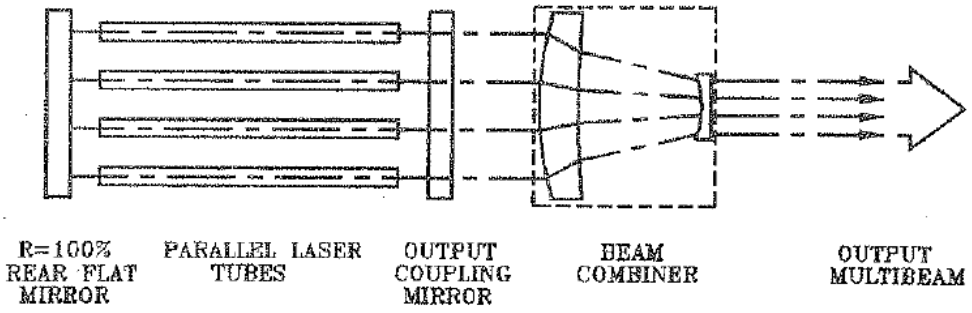

Figure 3. Schematic diagram of a multibeam laser.

Design considerations of a Class I CO_2 Laser

Output power of a typical Class I CO_2 laser operating in an optimized condition with respect to gas ratio, pressure, and tube current may be calculated if design data on the optical cavity and laser tube are known. This section presents a set of equations that may be used to determine approximate maximum output power of a Class I CO_2 laser. The equations are based in part on experimental observation and are presented without a theoretical development. An example problem is included to illustrate use of the equations.

Design Equations

The following can be used to determine output power of a CO_2 laser:

$$P(W) = \frac{8.36\,[(1-\ell)^{1/2}T]\{aL_a + 1n[(1-\ell)(1-\ell-T)]^{1/2}\}}{\{(1-\ell)^{1/2} + (1-\ell-T)^{1/2}\} \times \{1-[(1-\ell)(1-\ell-T)]^{1/2}\}} \quad \textbf{...(1)}$$

$$\ell_d = e^{-\left(\frac{2r^2}{w_s^2}\right)} \quad \textbf{... (2)}$$

$$w_f^4 = \left(\frac{\lambda}{\pi}\right)^2 L_c(R - L_c) \quad \textbf{...(3)}$$

$$w_s^4 = \left(\frac{\lambda R}{\pi}\right)^2 \left[\left(\frac{R}{L_c}\right) - 1\right]^{-1} \quad \textbf{... (4)}$$

$$\ell_d = e^{-\frac{2\pi r^2}{R\lambda}\left(\frac{R}{L_c} - 1\right)^{1/2}} \quad \textbf{... (5)}$$

$$\alpha = (0.0822\ \text{cm}^{-1} - 0.0026\ D\ \text{cm}^{-2}) \quad \textbf{... (6)}$$

P = Output power of laser in watts (Equation 1).

l = Total cavity loss.

T = Fractional transmission of output coupler.

a = Gain coefficient (Equation 6).

L_a = Active length (length of discharge providing gain), in centimeters.

l_d = Diffraction loss of beam passing through an aperture (Equations 2 and 5).

r = Radius of cavity-limiting aperture.

W = Watts of power.

w = Spot size (radius to $\frac{1}{e^2}$ points) of beam at aperture.

w_f = Spot size (radius to $\frac{1}{e^2}$ points) of beam on flat mirror (Equation 3).

w_s = Spot size (radius to $\frac{1}{e^2}$) of beam on spherical mirror Equation 4).

R = Radius of curvature of spherical mirror, in meters.

L_c = Cavity length (distance between mirror surfaces), in meters.

D = Tube diameter, in centimeters.

λ= Laser wavelength.

Equation 1 gives the power of the laser during optimum operation if active length, gain coefficient, loss, and transmission of the output coupler are known. Transmission of the output coupler and the active length may be obtained from system data sheets or can be measured. The gain coefficient is given by Equation 6 in cm^{-1} where tube diameter D is measured in cm. Loss is calculated using either Equations 2 or 5 as described below.

Equation 2 gives the diffraction loss of a Gaussian laser beam of radius w when it passes through an aperture with a radius r. In this case the radius r is the radius of the cavity aperture, when is located near the spherical mirror, and beam radius w is defined as the spot size of the beam on that mirror.

Size of the Gaussian laser beam inside the optical cavity depends upon curvature and separation of the mirrors and the wavelength of the light. Size of the aperture does not affect size of the beam for any given laser mode. It determines only the loss for that mode. Equations 3 and 4 give spot sizes of the TEM_{00} mode on the flat and spherical mirrors for a long-radius hemispherical cavity.

Equation 5 is the result of substituting the value for w_s from Equation 4 into the expression for diffraction loss in Equation 2. Thus, Equation 5 gives the diffraction loss for any long-radius hemispherical laser cavity with its limiting aperture near the spherical mirror. This is usually the case, because the beam has its maximum diameter on the spherical mirror.

In CO_2 lasers the limiting aperture is usually the bore of the laser tube. Decreasing the bore increases gain because of more efficient gas cooling, but it also increases diffraction loss. Larger-diameter tubes also tend to support higher-order TEM modes. In most Class I CO_2 lasers tube diameter is chosen to give a loss of 2% to 15% for TEM_{00}, depending on laser size. If optics of the system are clean, undamaged, and aligned properly, total loss l usually may be assumed to be equal to the diffraction loss l_d. If damaged optics or additional optical components are present, the loss they introduce must be added to the diffraction loss.

The following example illustrates use of Equations 1 through 6 in determination of output power and beam diameter of a CO_2 laser.

Example: A CO2 laser with an active length of 2 m and a cavity length 2.4 m. Tube inner diameter is 12 mm. The output coupler is flat and has a transmission of 20%. The HR mirror has a radius of curvature of 5 m. The only significant loss l in the system is diffraction loss, l_d. Find Output power and diameter of output beam.

Solution:

Given quantities (in appropriate units) are:

L_a = 200 cm

L_c = 2.4 m

D = 1.2 cm

$r = \frac{D}{2} = 6 \times 10^{-3}$ m

$T = 0.20$

$R = 5$ m

From Equation 6, the gain coefficient is

$a = (0.0822\ \text{cm}^{-1} - 0.0026 \times D\ \text{cm}^{-2})$

$a = [(0.0822\ \text{cm}^{-1}) - (0.0026)(1.2\ \text{cm})(\text{cm}^{-2})]$

$a = 0.0791\ \text{cm}^{-1}$

Spot sizes of the beam on the two mirrors are determined using Equations 3 and 4

$$w_f^4 = \left(\frac{\lambda}{\pi}\right)^2 L_c(R - L_c)$$

$$= \left(\frac{10.6 \times 10^{-6}\ \text{m}}{\pi}\right)^2 (2.4\ \text{m})(5\ \text{m} - 2.4\ \text{m})$$

$w_f^4 = 7.104 \times 10^{-11}\ \text{m}^4$

$w_f = 2.90 \times 10^{-3}$ m

$$w_s^4 = \left(\frac{\lambda R}{\pi}\right)^2 \left[\left(\frac{R}{L_c}\right) - 1\right]^{-1}$$

$$= \left[\frac{(10.6 \times 10^{-6}\ \text{m} \times 5\ \text{m})}{\pi}\right]^2 \left[\left(\frac{5\ \text{m}}{2.4\ \text{m}}\right) - 1\right]^{-1}$$

$w_s^4 = 2.6272 \times 10^{-10}\ \text{m}^4$

$w_s = 4.026 \times 10^{-3}$ m

Output beam diameter is twice the spot size on the flat coupler (w_f).

Output beam diameter = 5.8 mm.

The diffraction loss may be calculated using Equation 2.

$$l_d = e^{-2r^2/w_s^2}$$

$$= e^{-\left[(2)(6 \times 10^{-3}\,\mathrm{m})^2 / (4.026 \times 10^{-3}\,\mathrm{m})^2\right]}$$

$$= e^{-}(4.44)$$

$l_d = 0.012 = 1.2\%$

Since the diffraction loss l_d is the only significant loss factor, total l loss may be assumed to be equal to l_d, or 1.2% Equation 1 now may be used to determine laser output power.

$$P = \frac{8.36\,[(1-\ell)^{1/2}\,T]\{\alpha L_a + \ln[(1-\ell)(1-\ell-T)]^{1/2}\}}{\{(1-\ell)^{1/2} + (1-\ell-T)^{1/2}\} \times \{1-[1-\ell)(1-\ell-T)]^{1/2}\}}$$

$(1 - l) = 1 - 0.012 + 0.988$

$(1 - l - T) = 1 - 0.012 - 0.20 = 0.788$

$$P = \frac{8.36\,[(0.988)^{1/2}\,(0.20)]\{(0.0791)(200) + \ln[(0.988)(0.788)]^{1/2}\}}{\{(0.988)^{1/2} + (0.788)^{1/2}\} \times \{1-[(0.988)(0.788)]^{1/2}\}}$$

$$= \frac{26.08}{0.221}$$

$P = 117.8$ watts

This laser will have an output beam diameter of 5.8 mm and a maximum output power of 118 W.

H.W.

Use laser parameters given in Example as a specific case to construct graphs showing variation of output power as other parameters are varied. In each case, assume that all parameters are fixed at the value stated in Example except for the parameter specified as variable. Draw a separate graph of output power versus each of the following:

a. Transmission of output coupler varies from 50% to 60%.

b. Tube bore varies from 10 mm to 16 mm.

c. Cavity length varies from 1.5 m to 2.5 m as active length varies from 1.1 m to 2.1 m.

FLASHLAMPS FOR PULSED LASERS AND FLASHLAMP POWER SUPPLIES

This lesson will introduce the student to the basic mechanical, optical, and electrical operation and concepts of flash lamps. Pulsed xenon and krypton flash lamps are used to convert electrical energy to optical radiation for pumping solid-state lasers and some dye lasers. Flash lamps are gas-discharge devices designed to produce pulsed radiation, unlike arc lamps, which are gas-discharge devices designed to produce continuous radiation.

The flash lamp is electrically pulsed to produce high values of radiation flux in a given spectral band. The type of flash lamp selected should be able to supply the maximum spectral output in the absorption bands of the laser material. Flash lamp specifications include lamp type and construction, arc length, bore diameter, gas-fill pressure, energy-handling capabilities, lifetime, and cooling requirements.

Figure 1 shows some typical lamp configurations. Linear flash lamps are in the form of straight tubes, with bore diameter of from 3 to 19 millimeters and a wall thickness of 1 to 2 millimeters. Lengths in the 5- to 10-centimeter region are common, but lamps as long as one meter are available.

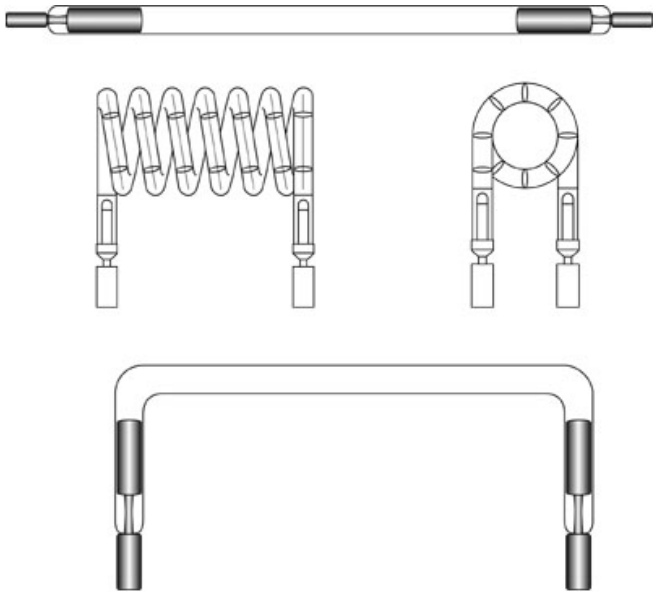

Fig.1 Flash lamp types.
Top (a): Linear flash lamp.
Middle (b): Helical flash lamp, side and end views.
Bottom (c): U-shaped flash lamp

The lamp is filled to a pressure usually in the range of 300 to 700 torr. The fill gas is most often xenon.

Electrical Characteristics of Flash lamps

All electrical discharges in gaseous media, including flashlamps and arc lamps, have common characteristics; The impedance characteristics of a flashlamp determine the energy-transfer efficiency from the capacitor bank to the lamp. The impedance is a function of time and current density. Flashlamp electrical characteristics can be discussed in three distinct areas of operation, which occur sequentially as the electrical discharge through the lamp develops.

The electrical characteristics of flashlamps are characterized by these three different operating regimes:

• Triggering and initial arc formation

• Unconfined discharge

• Wall-stabilized operation at high current.

The electrical resistance, *R(t)*, of a flashlamp as a function of time, *t*, is a function of the electrical current, *I(t)*, the lamp inside diameter, *d*, and the lamp length, *L*, between electrodes. The pulse shape for the current for a typical flashlamp pulse with duration of a few hundred microseconds is shown in Figure 2.

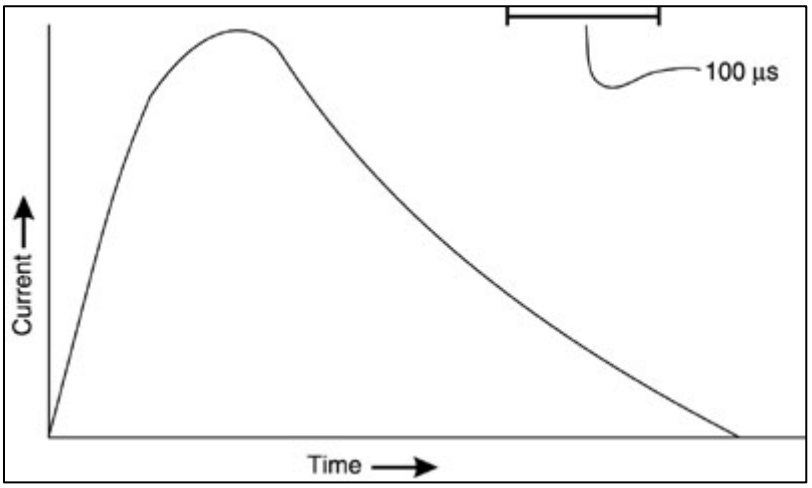

Fig. 2 Typical waveform for a flashlamp current pulse lasting a few hundred microseconds

Example B: Flashlamp Resistance	
Given:	A xenon flashlamp with an inner diameter of 12 mm and an arc length of 6 inches (15.24 cm). The resistivity of xenon is assumed to be 0.020 Ω -cm.
Find:	Resistance of the lamp.
Solution:	$R = \frac{\rho \ell}{A}, A = \pi r^2$ $= \frac{0.020\ \Omega - \text{cm})(15.24\ \text{cm})}{(3.14)(0.6\ \text{cm})^2} =$ $\frac{0.3048\ \Omega - \text{cm}^2}{1.131\ \text{cm}^2}$ $R = 0.27\ \square$

Power Supplies for Flashlamps

The power supply for a pulsed flashlamp performs a number of functions:

- Charges a capacitor that stores electrical charge until the flashlamp is ready to fire.
- Provides a trigger pulse that initiates the pulse.
- Controls the flow of current during the pulse to control the pulse shape.

Triggering

Four types of triggering circuits have commonly been used as circuitry to trigger the flashlamp:

• Over-voltage

• External

• Series

• Parallel

The last three are used most often with solid-state lasers. The advantages and disadvantages of the triggering mechanisms will be discussed.

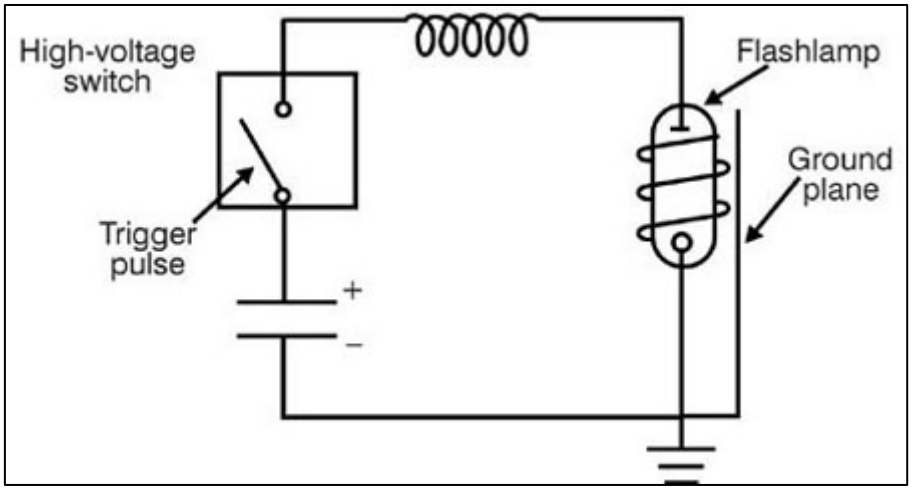

Fig. 1 Over voltage trigger circuit

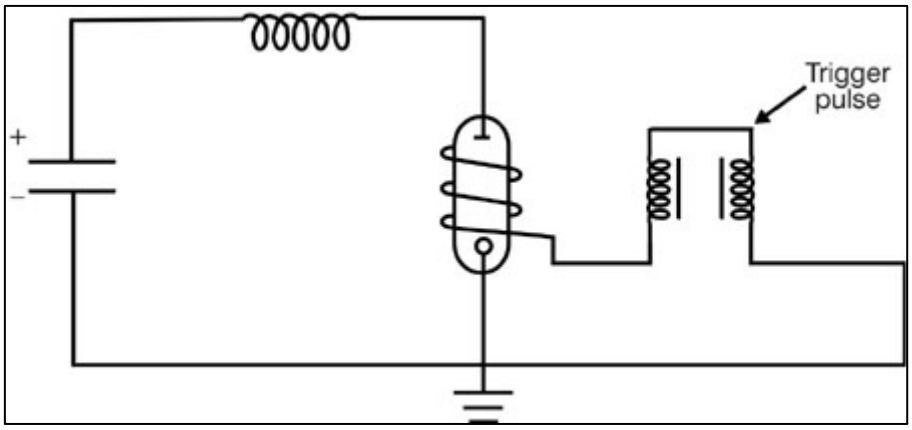

Fig. 2 External trigger circuit

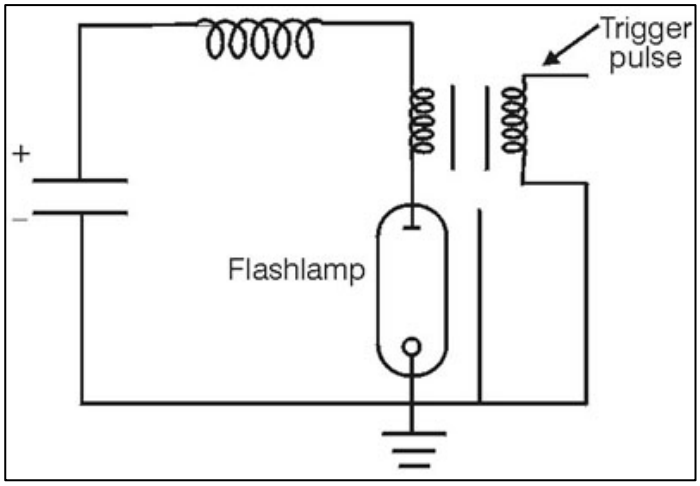

Fig. 3 Series trigger circuit

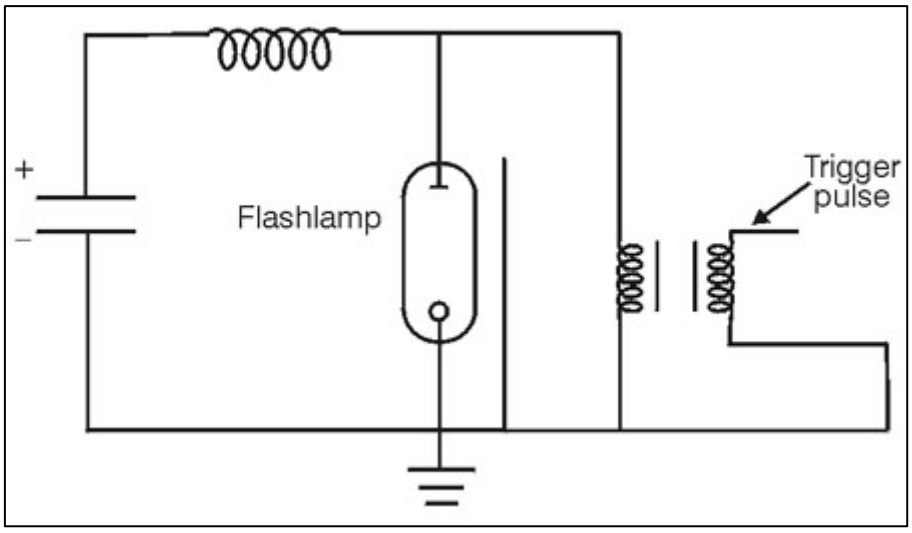

Fig. 4 Parallel trigger circuit

In addition, reliable triggering requires the use of a ground plane near the flashlamp. This is a factor independent of the method of triggering. Often, this stable voltage reference is a wire wrapped around the lamp. The entire arc length should be spanned to allow triggering to occur at the lowest values of voltage. The presence of the ground plane is indicated in the figures above.

H.W, given a two-inch arc length, how long should the trigger pulse be?

Control of Pulse Shape

The function of pulse forming network is to stores energy and deliver it to the lamp in desired pulse current shape. The pulse-shaping circuit shown in Figure 5 is an RLC discharge circuit. It consists of a single

capacitor for energy storage, a single inductor for pulse shaping, and a resistive load in the form of the flashlamp.

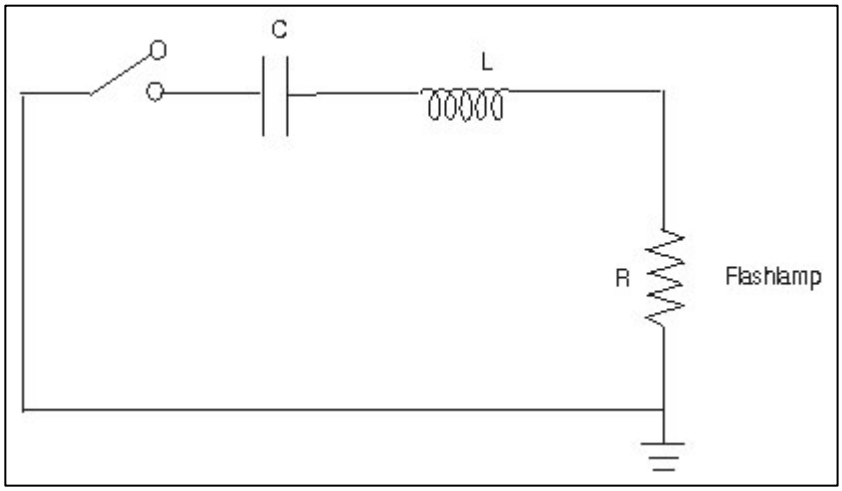

Fig. 5 RLC discharge circuit

The values of (RLC) may be obtained from the following equations:

$$C = (0.09 \text{ x } E_0 \text{ x } t_p^2/K_0^4)^{1/3} \qquad \ldots(1)$$

$$L = t_p^2/9C \qquad \ldots(2)$$

$$V = (2E_0/C)^{1/2} \qquad \ldots(3)$$

As an example, consider a flashlamp with a lamp-impedance parameter of 13 ohm-ampere$^{1/2}$. One desires to discharge 100 joules of energy through this lamp in a pulse of 500-microseconds duration. According to Equation 18 the capacitance should be $C = [0.09 \text{ x } 100 \text{ x } (500 \text{ x } 10^{-6})2/(13)4]^{1/3} = 0.199 \text{ x } 10^{-3}$ farads = 199 microfarads.

Then the inductance $L = (500 \text{ x } 10^{-6})2/(9 \text{ x } 0.199 \text{ x } 10^{-3}) = 1.40 \text{ x } 10^{-4}$ henry = 140 microhenrys.

Finally, the voltage $V = (2 \text{ x } 100/0.199 \text{ x } 10^{-3})^{1/2} = 1002$ volts.

The pulse circuit described above has a single inductor and a single capacitor and is referred to as a single-mesh network. In many cases, the circuit will contain two or more *LC* networks in series. This situation is called a multiple-mesh network. This is illustrated in Figure 6, for the case of three meshes.

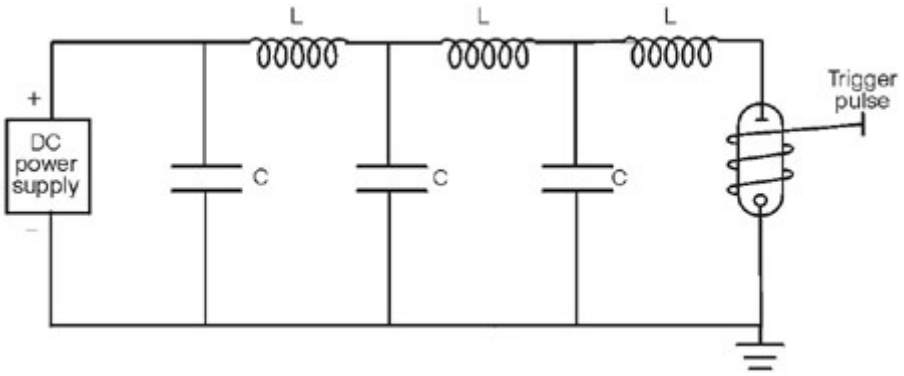

Fig. 6 Multiple-mesh discharge circuit

H.W: A 5ms- long current pulse is desired for two linear lamps connected in series and pumped at a total energy input of (1KJ). Each of lamps has an arc-length of (10cm) and a bore of (1cm). If we assume a peak current of (i_p=650A). Design a multiple mesh network including number of LC sections, inductance and capacitance per section and capacitor voltage.

Simmer Mode and Pseudosimmer Mode Circuits

Many pulsed solid-state laser systems incorporate driving circuits known as "simmer mode" or "pseudosimmer mode" circuits. These circuits maintain a steady-state partial ionization of the lamp during the time the lamp is not flashing. This is done by establishing and maintaining a low-current DC arc between the lamp electrodes. These circuits offer many operational advantages.

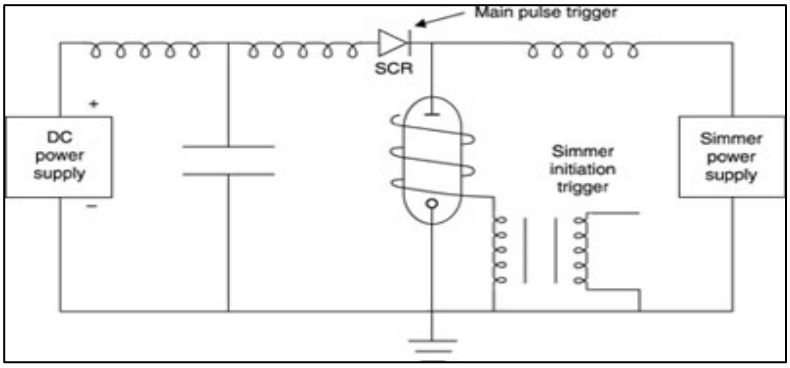

Fig. 7 Circuit for simmer mode operation

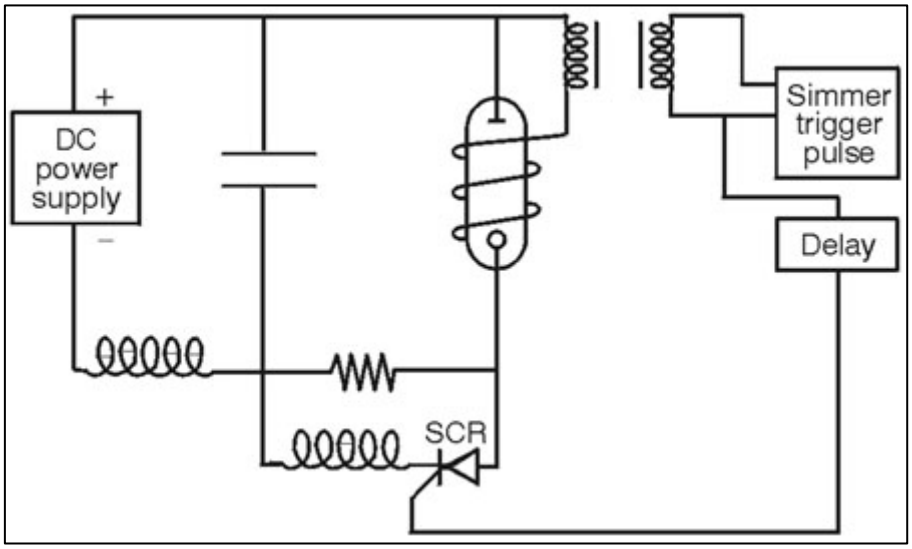

Fig. 8 Circuit for pseudosimmer mode operation

Optical Characteristics

The light emitted from flashlamps contains both discrete line structure and continuum radiation. The line structure arises from transitions between energy levels of the atoms and ions in the discharge. The continuum radiation is blackbody radiation, characteristic of the temperature of the plasma in the discharge. The exact spectral content is complicated, depending in a complex way on the gas type and pressure, the current, the plasma temperature, and the electron density. In addition, the spectral content of the light can change during the course of the pulse.

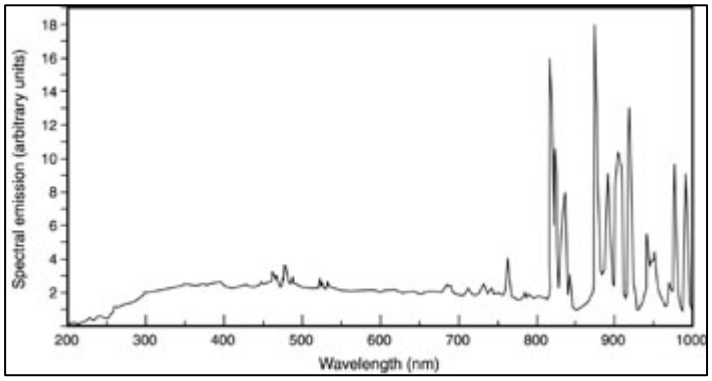

Fig. 1 Spectral emission from xenon flashlamp filled to a pressure of 390 torr at low electrical loading (100-microfarad capacitor charged to 500 V).

The conversion of the electrical input energy to optical radiant energy can be high, often in the 40-60% range for xenon and in the 25-30% range for krypton. Because of the higher efficiency, xenon gas fills are preferred for many applications.

The output of the flashlamp emerges through the envelope. The spectral absorption of the envelope will affect the spectral content. Most often the envelope is fused silica (silicon dioxide, also called fused quartz).

Mechanical Characteristics

Important considerations in the structure of flashlamps include the envelope, the electrodes, and the seal of the electrodes to the envelope.

The material used as the envelope for flashlamps for laser-pumping applications is silica fused quartz, also known as vitreous silica or fused quartz.

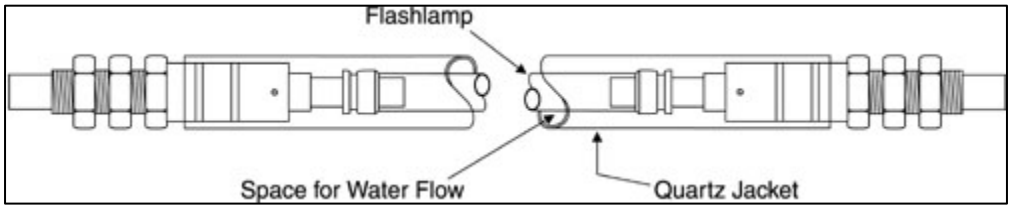

Fig. 2 Diagram of liquid-cooled flashlamp showing outer quartz jacket

The electrodes in flashlamps must withstand high temperature and high electrical-current density. Because of the high melting temperature of tungsten, some form of tungsten is used.

There are two commonly used structures for sealing the electrodes into the quartz tubes for flashlamps: tungsten rod seals and end cap seals, also called solder seals.

Cooling for Flashlamps

The main goal of lamp cooling is to keep acceptable average temperatures for the lamp electrodes and internal envelope surface. When the temperature in these regions exceeds safe values, lamp lifetime is reduced because of erosion of material. Sputtering of the electrodes and vaporization of the inside surface of the quartz envelope result from exceeding safe temperature values. Other effects of overheating include buildup of stress in the lamp envelope. This may lead to bending or fracturing of the envelope.

Failure Mechanisms and Lifetime

The lifetime of a flashlamp is rated according to the number of "shots" or discharges it will undergo before it is no longer operable, or until its output light level drops below an acceptable level. Lifetime varies with pulse duration, peak loading of the lamp, and rise time of the current pulse. Lamp failure is characterized by either a catastrophic explosion or fracturing of the lamp envelope, or by a gradual lowering of the output (that is, due to absorption of light inside the lamp).

Figure 3 is a graph of explosion energy per inch of arc length versus pulse duration for linear xenon flashlamps. Lines that indicate explosion energies of seven different lamp diameters are shown. The vertical scale is calibrated in joules of explosion energy per inch of arc length. The horizontal scale is in

seconds of pulse duration, with pulse duration defined as the full width of the pulse at one-third the maximum power.

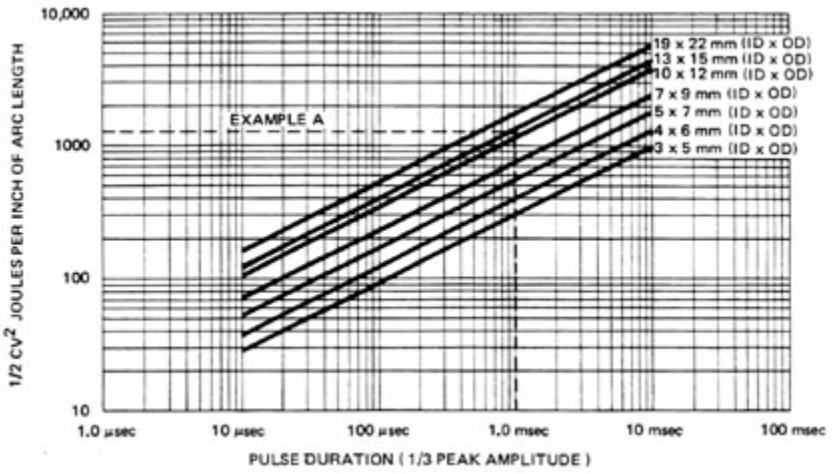

Fig. 3 Explosion energy per inch of arc length versus pulse duration for several Xe-filled lamp diameters.

CW Nd:YAG LASER SYSTEMS

Introduction

Several solid-state laser systems may be operated continuously, but the most common of these is the CW Nd:YAG laser system, operating at 1.06 microns. This lecture discusses the basic components, general characteristics, and subsystems of these lasers. As the removal of waste heat energy is of the greatest importance in the solid-state laser systems, and in particular in CW systems, much of this lecture will deal with energy flow in the laser and with cooling considerations.

This lecture explains the efficiency of a CW Nd:YAG laser by analyzing the power flow and conversion through each component of the system. The purpose of this exercise is to illustrate where power losses can occur, which elements of the laser will become excessively hot during operation, and what methods are useful to cool these components.

Components of a CW Nd:YAG Laser

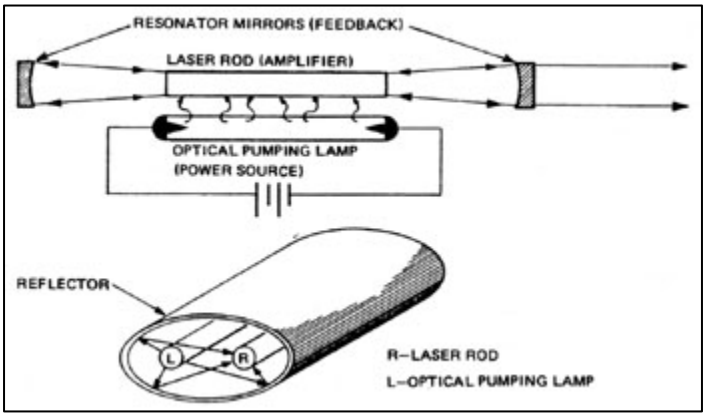

Fig. 1 Basic design of CW Nd:YAG lasers.

Laser Rod

Optical Pumping System

Optical Cavity

Cooling System

The cooling system is one of the most critical subsystems in the laser. Smaller lasers may use open-loop cooling systems with tap water flowing across the rod. In such cases, the water should be filtered to remove any contamination or impurities. Larger systems use closed-loop cooling with water or a water-glycol solution. The coolant is usually refrigerated, but water-to-water or water-to-air heat exchanger may also be employed.

Energy Losses in Nd:YAG Lasers

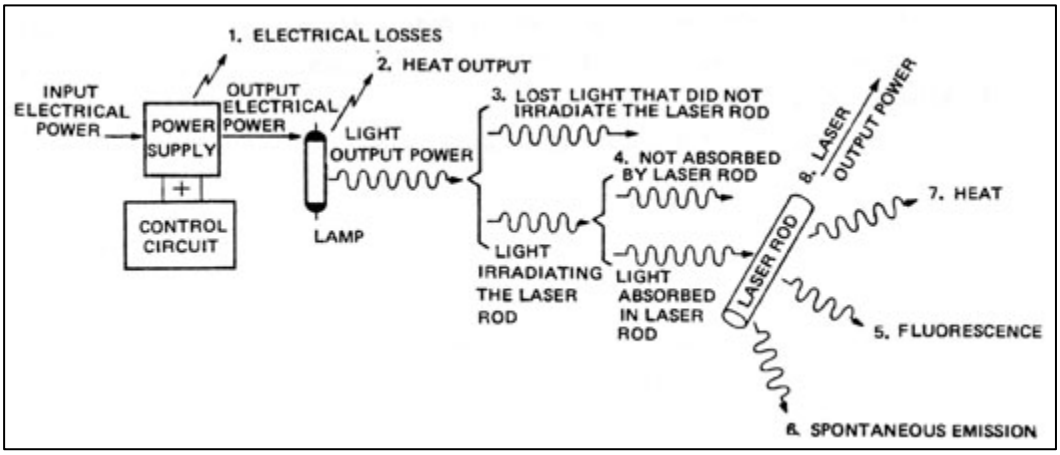

Fig. 2 CW solid-state laser efficiency diagram.

Cooling System Calculations

The cooling system of the laser must remove most of the waste heat from the entire system. Only a small fraction of the input energy appears in the laser output. Other relatively small amounts of energy escape as fluorescence passing through the rod ends and as radiative or convective heating of the laser environment. The cooling system must be capable of removing waste heat continuously at the maximum input power level.

Example A: Cooling System Design for Nd:YAG Laser.	
Given:	A CW Nd:YAG laser with 1000 watts of electrical power input to a tungsten lamp requires a cooling system which will limit the

	temperature rise in the rod coolant to 3 centigrade degrees.
Find:	Water flow rate and total temperature rise in cooling water.
Solution:	*Step 1*: Estimate the amount of power absorbed by the rod. a. Power supply losses can be measured. (For this problem, assume that the power supply is 80% efficient). b. Percentage of lamp output (incident on the rod) absorbed by the laser can be estimated by comparing the output spectra with the absorption spectra of the rod. (For this problem, assume that 30% of the output is absorbed). c. Assume that the pump lamp reflector is 90% efficient. Total power absorbed in laser rod = (1000 watts) × (0.8) ×(0.30) × (0.9) = 216 watts *Step 2*: Estimate laser rod heat power to be removed (H_{LR}). a. Total power absorbed = 216 watts b. Output laser power = 7 watts H_{LR} = 216 – 7 = 209 watts *Step 3*: Convert units of heat power from watts to calories/second. H_{LR} = 209 watts 1 watt = $\frac{\text{joule}}{\text{sec}}$ H_{LR} = 209 joules/sec 1 calorie = 4.18 joules

$H_{LR} = \frac{209}{4.18} = 50$ cal/sec

Step 4: Determine flow rate. We know that 1 calorie will raise 1 gram of water (or approximately 1 cm^3) 1 degree centigrade. To limit temperature rise in the coolant water to 3 centigrade degrees, dissipating a heat rate of 50 calories/second, the heat exchanger must have a flow rate of $\frac{50}{3}$ cm3 /sec = 16.7 cm3 /sec = 1000 cm^3 /min or 0.26 gal/min.

Step 5: Determine total temperature rise in coolant water. After the water has cooled the laser rod, it must cool the lamp and cavity.

Total heat to be dissipated in coolant (H_{TOT}):

$H_{TOT} = P_{in}$ – power supply losses – laser output

H_{TOT} = 1000 – 200 – 7 = 793 watts

$H_{TOT} = 793 \frac{\text{joules}}{\text{sec}} = 189.7$ cal/sec

Flow rate = 16.7 cm3 /sec

Temperature rise = $\frac{H_{TOT}}{\text{Flow Rate}} = \frac{189.7 \text{ cal/sec}}{16.7 \text{ cm}^3/\text{sec}}$

= 11.4 cal/cm3 – 11.4 C?

Temperature rise in coolant = 11.4 centigrade degrees

The absolute equilibrium input temperature of the coolant water will be determined by characteristics of the cooling system and the ambient conditions.

A typical coolant temperature might be 40C^{o}. Using this value and those calculated in Example A, a coolant flow diagram can be drawn as shown in Figure 7.

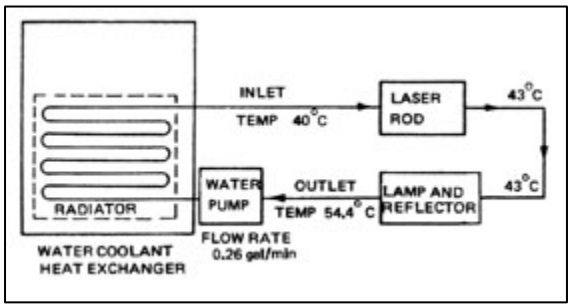

Fig. 3 Typical CW laser coolant flow diagram (parameter values obtained from Example A).

Active Resonator

In this section we will analyze the changes that occur if a lasing medium is inserted into the resonator. In CW and high-average-power solid state lasers the dominant effect that distorts the mode structure in a resonator is thermal lensing. Heat removed from the rod surface generates a thermal gradient.

The thermally induced spatial variations of the refractive index cause the laser rod to act as a positive lens with a focal length that depends on the power dissipated as heat from the pump source.

Resonator Containing a Thin Lens. We will analyze the case of a resonator containing an internal thin lens. To a first approximation, this lens can be thought of as representing the thermal lensing introduced by the laser rod.

Beam properties of resonators containing internal optical elements are described in terms of an equivalent resonator composed of only two mirrors. The pertinent parameters of a resonator equivalent to one with an internal thin lens are

$$g_1 = 1 - \frac{L_2}{f} - \frac{L_0}{R_1}, \quad g_2 = 1 - \frac{L_1}{f} - \frac{L_0}{R_2}, \qquad \ldots (1)$$

where $L_0 = L_1 + L_2 - (L_1 L_2 / f)$ and f is the focal length of the internal lens; L_1 and L_2 are the spacings between mirrorsM_1,M_2 and the lens, as shown in Fig.2a. The stability condition remains unchanged.

For the subsequent discussions we find it convenient to express the spot sizes in terms of g_1 and g_2. By combining R_1, R_2, and L with the relevant g_1 and g_2 parameters, can be written

$$w_1^2 = \frac{\lambda L}{\pi}\left[\frac{g_2}{g_1(1-g_1g_2)}\right]^{1/2},$$
$$w_2^2 = \frac{\lambda L}{\pi}\left[\frac{g_1}{g_2(1-g_1g_2)}\right]^{1/2}. \qquad \ldots (2)$$

From (2) follows

$$w_1^2 / w_2^2 = g_2 / g_1. \qquad \ldots (6)$$

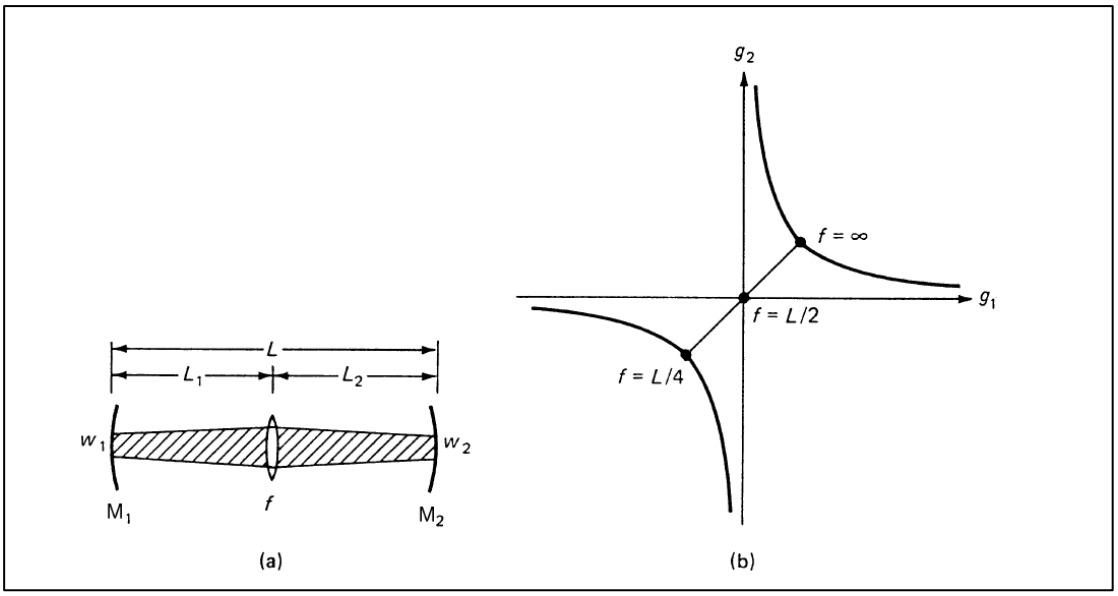

Fig.1 (a) Geometry and (b) stability diagram of a resonator containing a thin positive lens

As an example we will consider a resonator with flat mirrors (R_1 = R_2 =∞) and a thin lens in the center (L_1 = L_2 = L/2). From (1) and (2) we obtain

$$g = g_1 = g_2 = 1 - \frac{L}{2f}, \quad w_1^2 = w_2^2 = \left(\frac{\lambda L}{\pi}\right)(1 - g^2)^{-1/2}. \qquad \ldots (3)$$

For f =∞the resonator configuration is plane–parallel; for f = L/2 we obtain the equivalent of a confocal resonator; and for f = L/4 the resonator corresponds to a concentric configuration.

The mode size in the resonator will grow to infinity as the mirror separation approaches four times the focal length of the laser rod. Figure 2b shows the location of a plane–parallel resonator with an internal lens of variable focal length in the stability diagram.

Resonator Sensitivity to Mirror Misalignment.

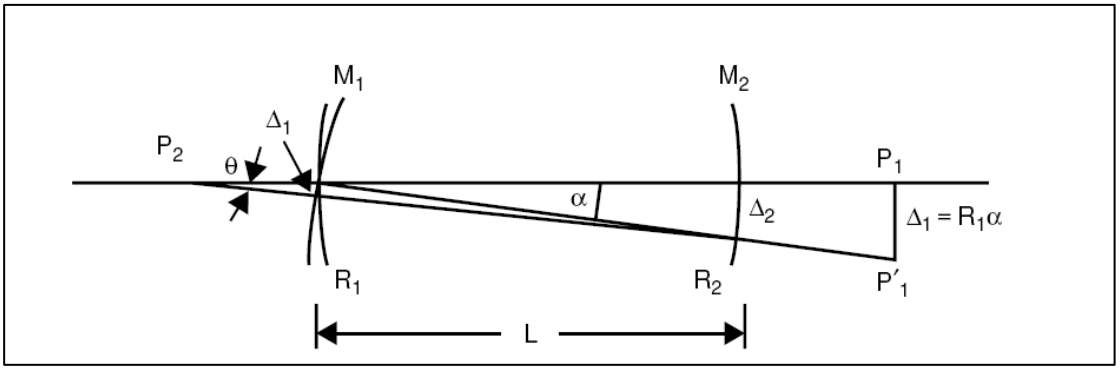

Fig.3 Misalignment of mirror M_1

If mirror M_1 is titled by an angle α, the center of curvature of mirror M_1 moves by $\Delta_1 = R_1\alpha$ to point P'_1. The resonator axis is rotated by an angle θ and the center of the mode pattern is shifted by Δ_1 and Δ_2 at mirror M_1 and M_2, respectively. From geometric considerations one obtains

$$\Delta_1 = \frac{R_1(R_2 - L)}{R_1 + R_2 - L}\,\theta \qquad \Delta_2 = \frac{R_1 R_2}{R_1 + R_2 - L}\,\theta \qquad \ldots (4)$$

We can establish the following criteria for the design of an efficient and practical laser system emitting a high-quality beam:

– The diameter of the TEM00 mode should be limited by the active material.
– The resonator should be dynamically stable, i.e., insensitive to pump-induced fluctuations of the rod's focal length.
– The resonator modes should be fairly insensitive to mechanical misalignments.

H.W

- Consider the lamp-pumped Nd:YAG laser shown in fig. The pumping beam induces a thermal lens of focal length (f) in the rod. Assume that the rod is simulated by a thin lens of focal length (f=25cm) placed at the resonator center. Calculate the TEM_{00} mode spot size at the lens and at the mirror locations.

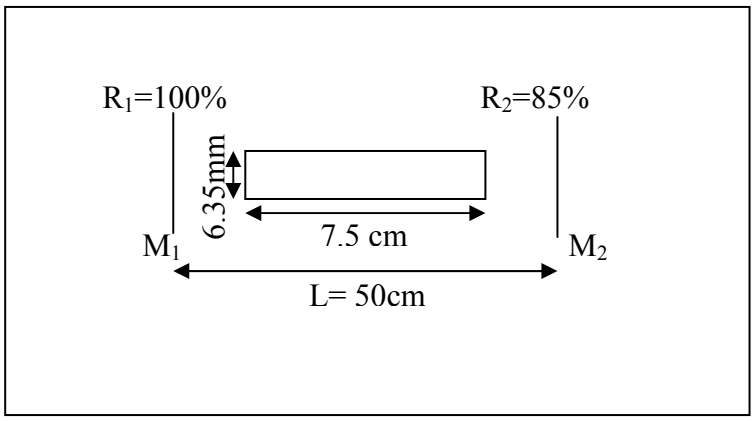

Fig.1

- Due to its relatively small sensitive to mirror misalignment a nearly hemispherical resonator (plane-spherical resonator) with $R=L+\Delta$ and ($\Delta<<L$) is often used for He-Ne laser at $\lambda=630nm$, if the cavity length (L=30cm) calculate:
  1. The radius of curvature of the spherical mirror, so that the spot size at this mirror is (0.5mm).
  2. The location in g_1-g_2 plane corresponding to this resonator.
  3. The spot size at the plane mirror.

Mode Selection

In general, the spot size of the TEM_{00} mode is relatively small. For example, a symmetric resonator with $R = 2$ m and $L = 1$ m has a radius of the TEM_{00} mode of $w_0 = 0.5$ mm at a wavelength of 1.06 μm. If the transverse dimension of the gain region of the active material is larger than the TEM_{00} mode dimension, a laser oscillator will typically operate in an incoherent superposition of several modes.

Many applications of solid-state lasers require operation of the laser at the TEM_{00} mode since this mode produces the smallest beam divergence, the highest power density, and hence the highest brightness. Furthermore, the radial profile of theTEM_{00} mode is smooth.

A large amount of research has been devoted to the design of optical resonator configurations that maximize energy extraction from solid-state lasers at the TEM00 mode. One finds that a resonator designed for TEM00 mode operation will represent a compromise between the conflicting goals of large mode radius, insensitivity to perturbation, good mode discrimination, and compact resonator length.

Insertion of an Intracavity Aperture.

With a properly sized intracavity aperture higher order modes can be suppressed and the laser can be forced to operate at the TEM00 mode but at the cost of substantially reduced output power and efficiency.

The diffraction losses caused by a given aperture and the transverse mode selectivity achievable with an aperture of radius (a) is illustrated in Fig. 1.

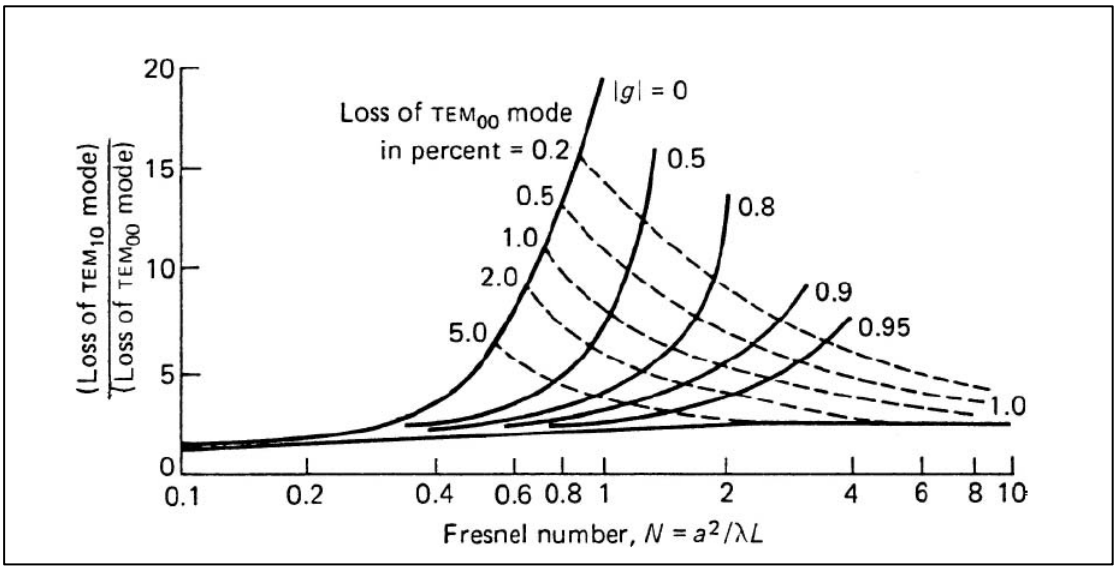

Fig.1. Ratio of the losses per transit of the two lowest order modes for the symmetrical resonator. The dashed curves are contours of constant loss for the TEM00 mode

Increasing Mode Size: Because the TEM00 mode has the smallest beam diameter of all the resonator modes, a number of techniques have been developed to increase the TEM00 mode volume in the active material, which is normally considerably larger in diameter than the mode size. One obvious solution to increase the TEM00 mode volume is to make the resonator as long as physical constraints permit, since for a given Fresnel number, the mode cross-sectional area increases proportional with length. Another approach is to utilize resonators, such as the concentric and hemispherical configuration. These resonators, owing to their focusing action, support large mode size differences along the axis. For example, in a hemispherical cavity the spot size in the limit can theoretically become zero at the flat mirror and grow to infinity for L = R. Location of the laser rod close to the curved mirror permits utilization of a large active volume as indicated in Fig.2.

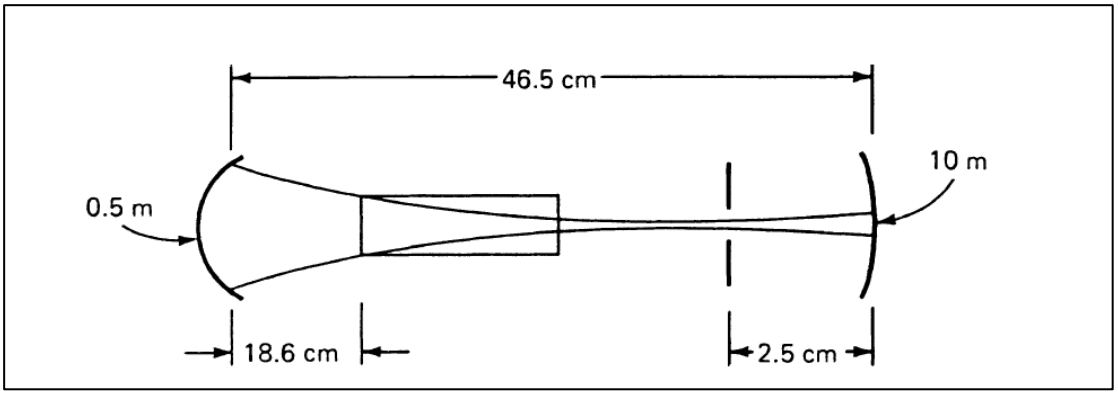

Fig.2 Focusing resonator geometry

Spatial Match of Gain Region and TEM00 Mode. In the end-pumped lasers the most elegant solution to the problem of mode selection can be implemented, namely a spatial match between the pump beam and the resonator TEM00 mode. Because the beam characteristics of diode lasers allow for tight focusing of their output radiation into the active material, a near-perfect overlap between the pump or gain region and the TEM00 mode volume can be achieved. Typically, the pump beam and resonator axis are oriented collinear within the active material. This way highly efficient TEM00 mode operation can be achieved.

Concave–Convex Resonator for a Weakly Focusing Laser Rod:
We concluded that with a convex mirror at one end of the resonator one can achieve $g1/g2 > 1$ and independently set $g1g2 = 0.5$. The first condition provides a large spot size $w2$ on mirrorM2, and the second condition minimizes the resonator sensitivity to changes of focal length. Another advantage of a concave resonator is its compactness in comparison with other resonators. Figure (4) illustrates a typical configuration consisting of a short-radius convex mirror at one end of the resonator, and a concave mirror at the other end of the laser rod close to it.

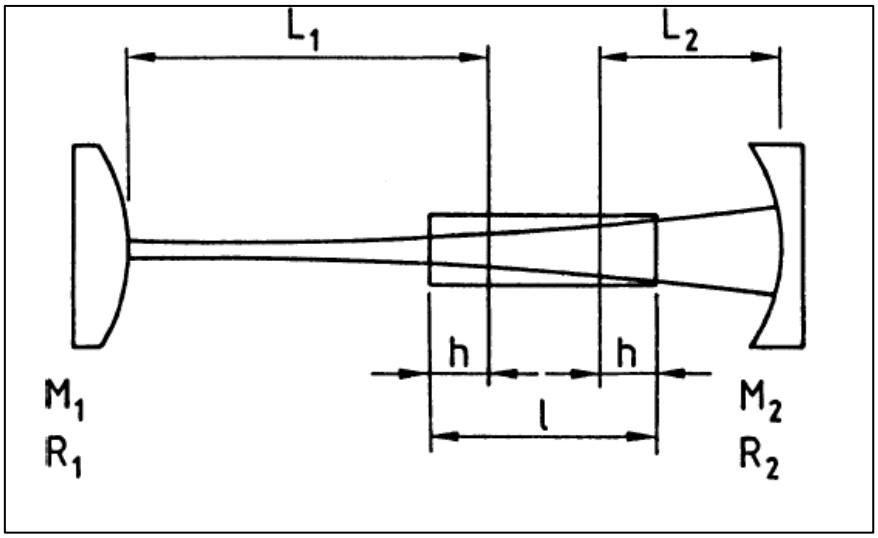

Concave–convex resonator containing a Nd:YAG rod

As an example we will calculate the parameters for a concave–convex resonator that has been used for a high repetition rate Nd:YAG laser. The laser rod, with a diameter of 5 mm, was measured to have a focal length of 6 m for a particular input. The length of the cavity was restricted to about 0.8 m. The optimum value of $w2$ has been found empirically to be equal to one-half the laser rod radius. With the rod as close as possible to the output mirror, the following design parameters are obtained for the equivalent resonator

$$w_2 = 1.25 \text{ mm}, \quad f = 6 \text{ m}, \quad L_1 = 0.7 \text{ m}, \quad L_2 = 0.1 \text{ m}.$$

We obtain a value of $g1 = 2.9$, and $g2 = 0.17$. The spot size on the concave mirror has a value of $w1 = 0.31$ mm. The curvatures of the mirrors can be as follows: The radius of the convex mirror is $R = -0.41$m and the concave mirror has a radius of $R = 1.1$m. The physical length of the resonator will be 82.25 cm for a 5-cm-long Nd:YAG crystal.

The design parameters for this particular laser cavity illustrate one disadvantage of the concave-convex resonator, namely, a very small spot size at the concave mirror.
This small spot size, which could lead to mirror damage, effectively precludes the use of this resonator in high-power Q-switched lasers.

Unstable Resonators

In a stable resonator the radiation is confined between the surfaces of the resonator mirrors. In order to produce a diffraction-limited output beam from a stable resonator, the Fresnel number must be on the order of unity or smaller, otherwise sufficient discrimination against higher order modes cannot be achieved. For practical resonator lengths, this usually limits the diameter of the TEM_{00} mode to a few millimeters or less.

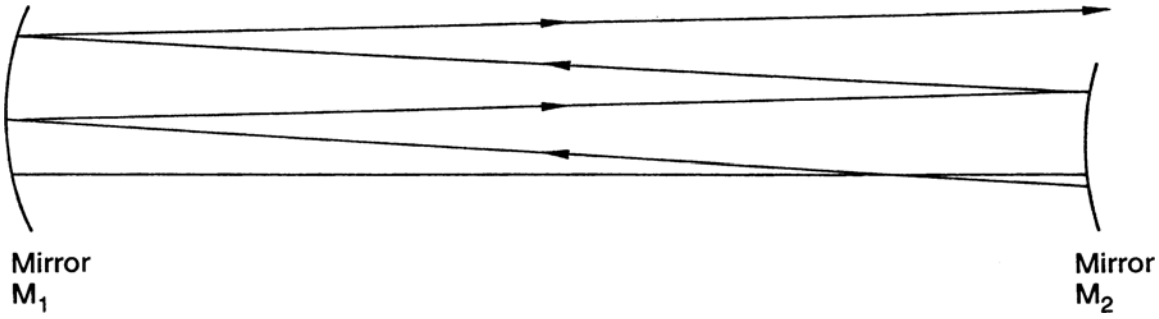

Fig.1. Light ray in an unstable resonator

About 10 years after its discovery, Byer and coworkers applied the unstable resonator concept for the first time to a Q-switched Nd:YAG oscillator/amplifier system. They did achieve a marked improvement in Nd:YAG output energy in a diffraction-limited mode.
However, only recently has the unstable resonator found applications in commercial lasers, mainly as a result of the availability of the variable reflectivity output mirror which provides a smooth and uniform output beam from an unstable resonator. Output coupling via such a mirror provides an elegant solution in overcoming the beam profile issue.

The most useful form of an unstable resonator is the confocal unstable resonator. A primary advantage of this configuration is that it automatically produces a collimated output beam; this also means that the final pass of the beam through the gain medium is collimated.

Confocal Positive-Branch Unstable Resonator

The confocal positive-branch unstable resonator is the most widely used form of the unstable resonator for solid-state lasers because it does not have

an intra-cavity focal point that could lead to air breakdown or could cause damage to optical components.

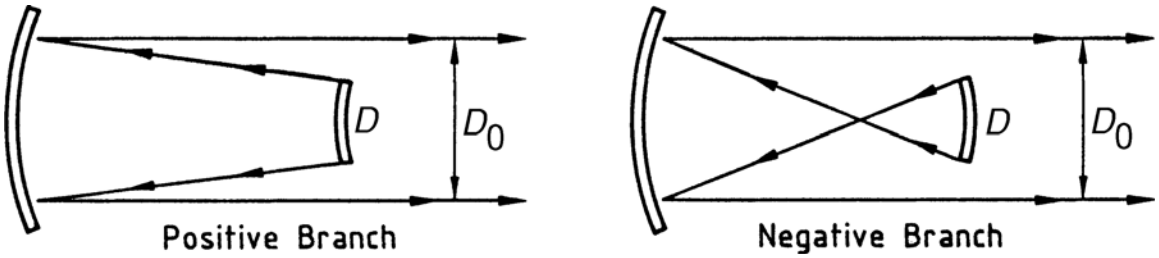

Fig.2 Positive and negative-branch confocal unstable resonator

If we insert the gain medium between the mirrors, the loss in energy has to be made up by the gain of the laser.

For a confocal resonator, the mirror radii are given by

$$R_1 = \frac{-2L}{M-1}, \qquad R_2 = \frac{2ML}{M-1} \quad \ldots (1)$$

Where L is the length of the resonator and R_1 and R_2 are the output and back-cavity mirror curvatures. Note that the output mirror has a negative curvature and thus is convex, while the rear mirror has a positive curvature and is concave.

The design depicted in Fig. 3 consists of a concave mirror M1 and a convex output mirror M2, both of which are totally reflecting. The dot mirror M2 is a small circular dielectrically coated area of radius *d* centered on a glass substrate.

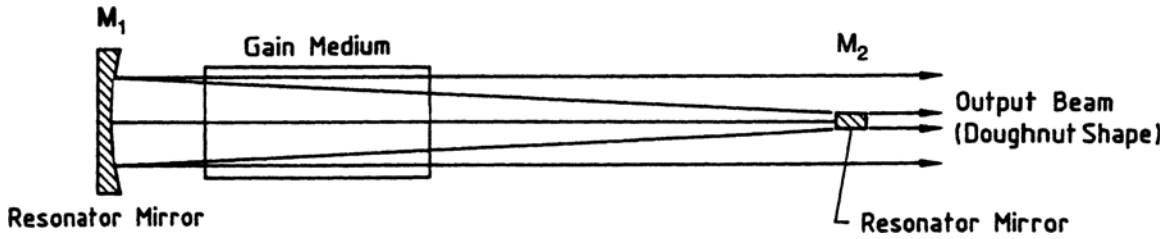

Negative-Branch Unstable Resonator

Fig.3 Small-mirror out-coupling scheme in a confocal, positive-branch unstable resonator

Because of the presence of an intra-cavity focal point, the negative-branch resonator has been neglected in practical laser applications. Despite the potential problem of air breakdown this resonator merits consideration owing to its unique feature of relatively large misalignment tolerances.

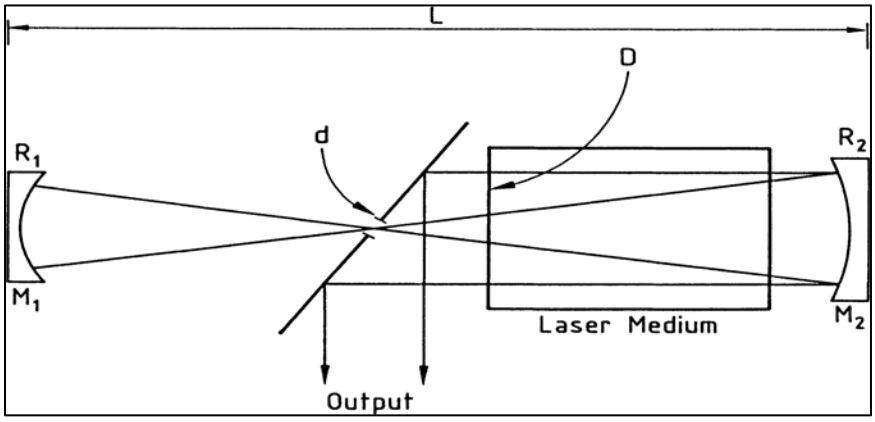

Fig.4 Arrangement of a typical negative-branch unstable resonator

The design parameters for a negative-branch resonator of the type shown in Fig. 6 are

$$R_1 = \frac{2L}{(M+1)} \quad \text{and} \quad R_2 = \frac{2ML}{(M+1)} \ldots (2)$$

where L is the confocal resonator length and M is the optical magnification defined before.

Variable Reflectivity Output Couplers

One of the major disadvantages of an unstable resonator, namely the generation of an annular output beam containing diffraction rings and a hot spot in the center, can be eliminated by employing a partially transparent output coupler with a radially variable reflectivity profile.

In such a mirror, reflectivity decreases radially from a peak in the center down to zero over a distance comparable to the diameter of the laser rod. Such a resonator is, in principle at least, capable of sustaining a single transverse mode of a very large volume and with a smooth, uniform spatial profile. Whether a large volume can be realized in a practical system depends on the gain of the system.

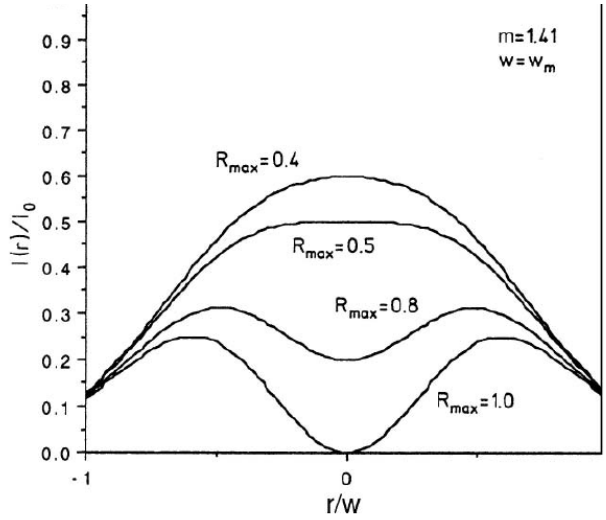

Fig.8 Profile of the output beam for various reflectivities of the mirror

Laser Diodes

The most efficient pump source for solid-state lasers is the diode laser. Although the advantage of pumping solid-state lasers with monochromatic pump sources has been recognized very early, the low power output, low packaging density, and extremely high cost of diode lasers prevented any serious application for laser pumping until the mid-1980s.

The major attributes of diode pumping can be summarized as follows:

- Increased system efficiency.
- Improved beam quality.
- Enabling technology for compact and versatile laser systems. - Enabling technology for new laser materials.
- Increased component lifetime.
- Benign operating features.
- Increased pulse repetition rate.

Spectral Properties

The spectral properties of laser-diode arrays that are most critical for the pumping of solid-state lasers are the center wavelength and the spectral width of the emission and the wavelength shift with temperature.

The wavelength of a laser diode is inversely proportional to the energy difference ΔE between the conduction and valence band

$$\lambda = hc/\Delta E, \qquad \ldots (1)$$

where h is the Planck's constant and c is the speed of light. The bandgap depends on the crystalline structure and chemical composition of the semiconductor.

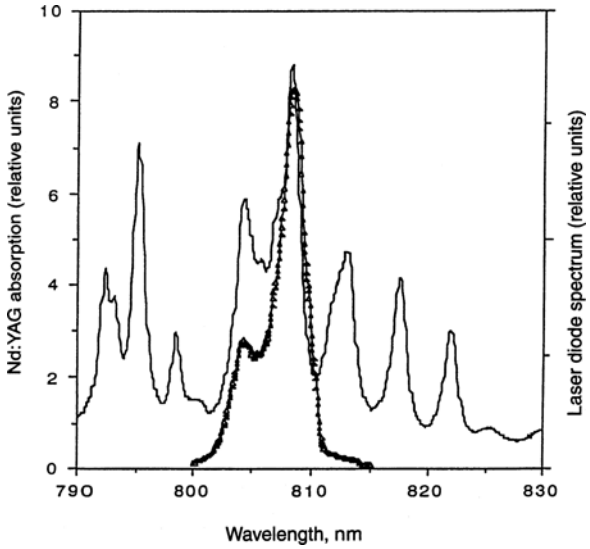

Spectral overlap between Nd:YAG absorption and emission spectrum of a 10 bar array

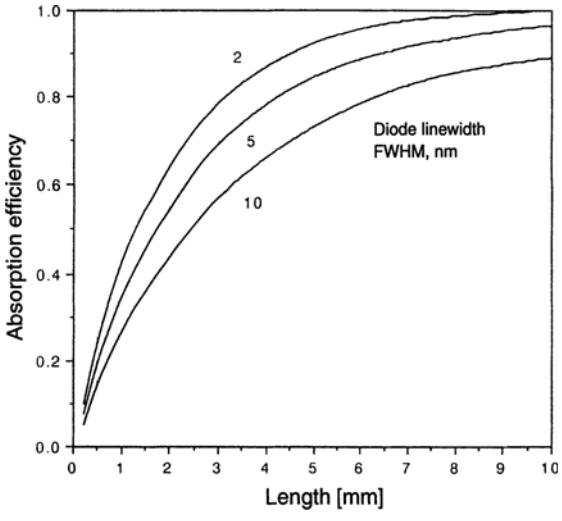

Absorption efficiency of Nd:YAG as a function of absorption length for a pump wavelength of 808 nm

In a GaAlAs structure the peak emission changes 0.3 nm/◦C. Therefore, the material composition has to be chosen such that the desired wavelength is achieved at the operating temperature of the junction.

The average temperature changes as a result of varying operating conditions of cw or high repetition rate diode pump sources can often be mitigated by temperature controlling the heat sink. In pulsed diode bars, the temperature rise during the pulse causes a change of the center wavelength, known as chirp, and a reduction of efficiency and output power, known as sag. This effect becomes particularly noticeable if a laser crystal with a narrow absorption width is pumped with a relatively long pump pulse. The transient temperature rise is determined by the heat sink properties.

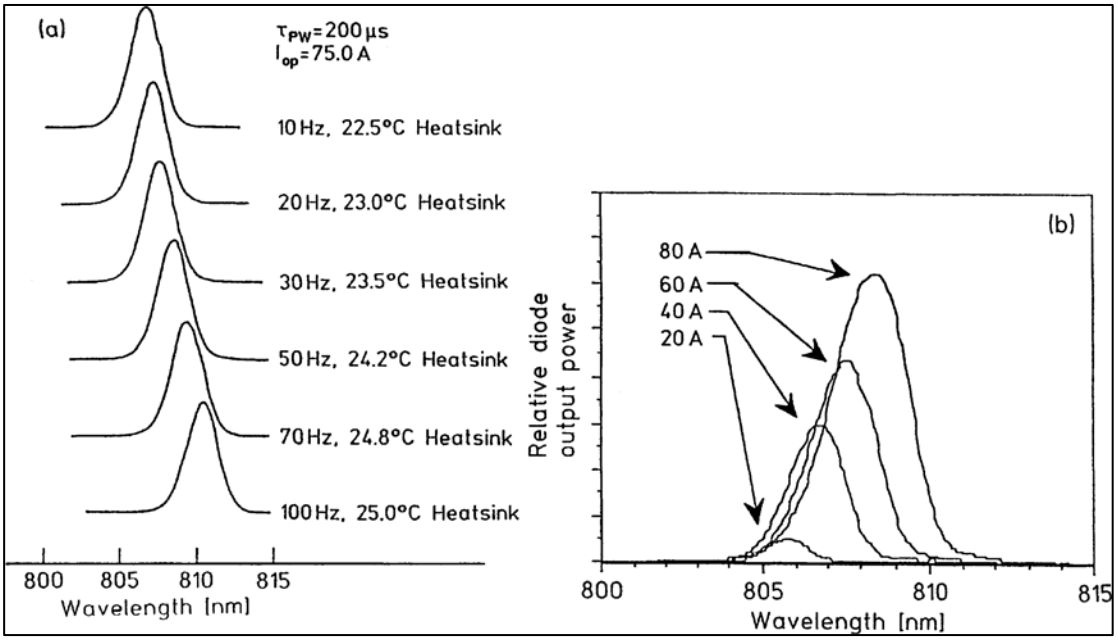

Fig.3 (a) Diode array linewidth vs. repetition rate and (b) wavelength shift vs. drive current

Laser diode pumps

There are four types of laser diode listed in order of increasing output power:

1. single strip
2. diode array
3. diode bar
4. stacked bars

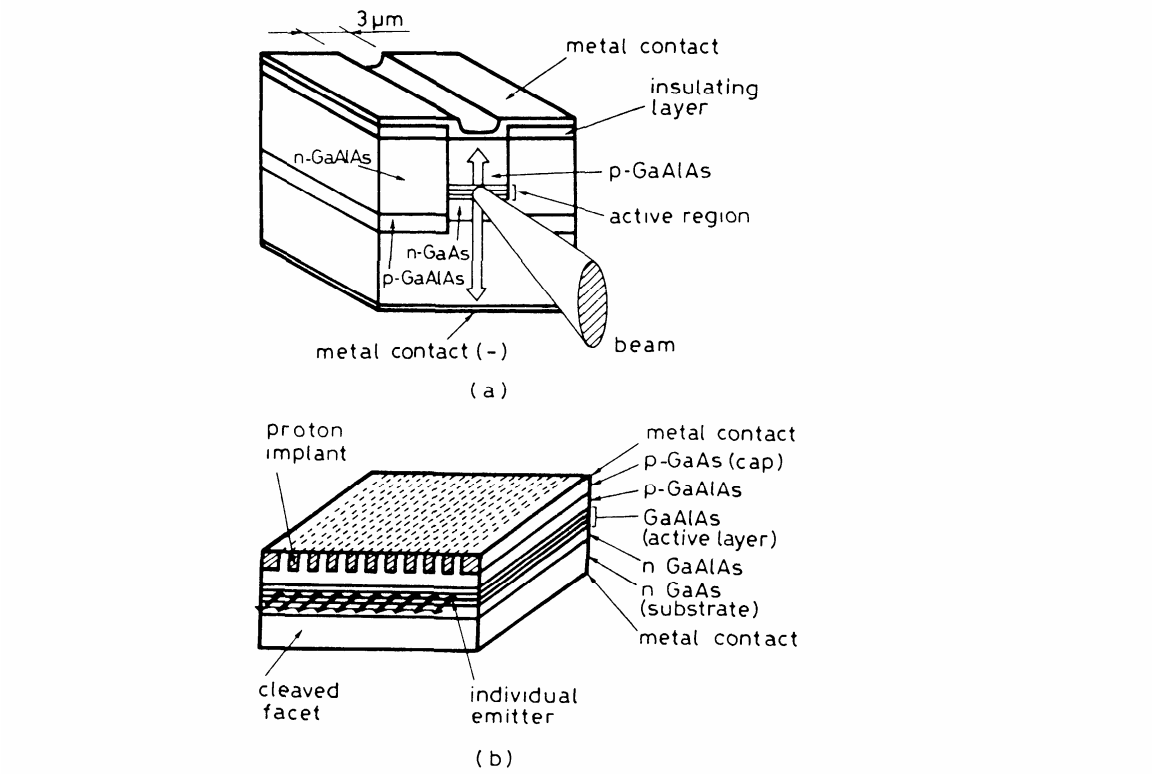

FIG. 6.9. (a) Single-stripe index-guided semiconductor diode laser and (b) monolithic array of many stripes on a single semiconductor chip.

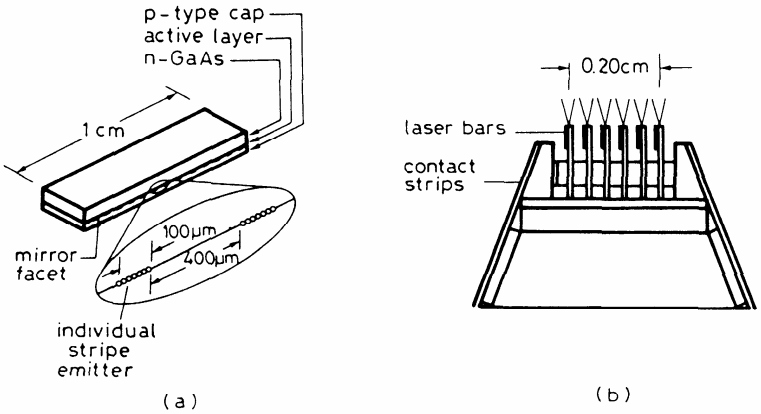

FIG. 6.10. (a) Monolithic 1-cm bar for cw operation and (b) stacked bars for quasi-cw operation.

6.3.2. Pump Transfer Systems

For efficient pumping, light emitted by the diode laser systems described above must be properly transferred to the active medium. There are basically two types of pump geometry: (1) *Longitudinal pumping*, where the pump beam enters the laser medium along the resonator axis. (2) *Transverse pumping*, where the beam is conveyed to the active medium, generally from one or more directions, transversely to the resonator axis. We consider the two cases separately because the corresponding diode lasers and pump-transfer systems are somewhat different.

6.3.2.1. Longitudinal Pumping

For longitudinal pumping, the beam emitted by the laser diode generally needs to be concentrated in a small (100 μm–1 mm diameter) and possibly circular spot in the active medium. Three of the most common laser configurations are shown in Figs. 6.11a–c. In Fig. 6.11a the laser rod is shown in a plane-concave resonator; the plane mirror is directly deposited on one rod face, with the pump beam focused on this face. In Fig. 6.11b–c two pump beams from two different diode systems are focused, on the rod center, from the two sides of the rod. The laser resonator can consist of either a folded ring configuration (Fig. 6.11b) or a z-shaped folded linear cavity (Fig. 6.11c). For these latter two configurations, the resonator axis is also indicated by a dashed line. Given these resonators, we now address the question of how to transform the pump beam into a possibly circular shape of the appropriate size within the laser rod.

We first consider the single-stripe configuration in Fig. 6.9a, which is used as a pump source for low-power devices. (Output powers up to several tens of mW can be achieved with single-stripe pumping.) The ellipticity of the strongly diverging beam of the diode

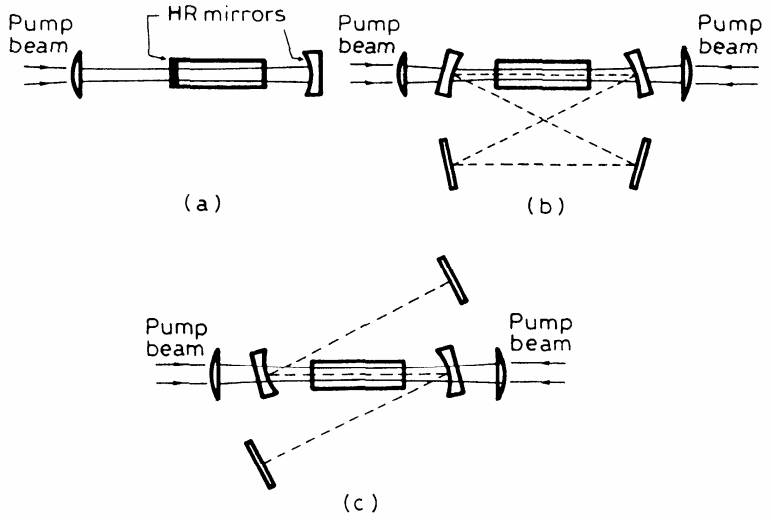

FIG. 6.11. Typical configurations for longitudinal diode laser pumping: (a) single-ended pumping in a simple plane-concave resonator, (b) double-ended pumping for a ring laser in a folded configuration, and (c) double-ended pumping for a z-shaped folded linear cavity.

In the case of a 200-μm-wide array, e.g., since divergence angles $\theta_\perp$ and $\theta_\parallel$ are approximately the same as for a single stripe, the configuration in Figs. 6.12a–c can still be used to produce a circular spot after the anamorphic prism-pair. Since the slow-axis beam divergence is however ~ 40 times larger than the diffraction limit, the spot at the focal plane of lens L_2 is elliptical, with a 40:1 ratio between the two axes. According to Example 6.2, for a well-corrected collimating lens L_1, the elliptical beam could be, e.g., 2.8 μm $\times$ 112 μm. In practice aberrations of the optical system, which are more pronounced for the fast-axis direction, tend to produce a more circular spot, with a spot size of perhaps 150 μm. Another widely used method, in diode arrays, for transferring a pump beam to the active medium involves the use of a multimode optical fiber. For a 200-μm stripe, a fiber with a 200-μm core diameter can be used with the fiber butt-coupled to the diode. With this configuration, however, the fiber numerical aperture NA ($NA = \sin\theta_f$, where θ_f is the acceptance angle of the fiber) must have a sufficiently high value to accept the highly diverging beam of the diode, i.e., $\sin\theta_f > \sin\theta_\perp \cong 0.4$. After propagation in a sufficient length of the fiber, the output beam becomes circular and its divergence is established by the fiber NA, i.e., one has $\theta_{out} = \theta_f$. During propagation along the fiber, the slow axis divergence is thus worsened from $\theta_{in} = \theta_\parallel$ to $\theta_{out} = \theta_f \cong \theta_\perp$. To reduce beam divergence, we can use a cylindrical lens of very short focal length, between array and fiber, to collimate the beam in the fast-axis direction to a diameter equal to the fiber diameter. We can then use a fiber whose NA approximately equals the slow-axis divergence, i.e., take $\theta_f \cong \theta_\parallel$. In this case, as shown in more detail in Example 6.3, the beam of a 200 μm wide array can be focused onto a fiber of perhaps 250–300 μm core diameter and NA of 0.1.

Example 6.3. *Diode-array beam focusing onto a multimode optical fiber.* We consider the simple configuration in Fig. 6.13, where a cylindrical lens of sufficiently short focal lens f is used to collimate the beam along the fast axis (*dashed lines*). The beam diameter after the lens and along this axis is then given by $D_\perp = 2f \tan\theta_\perp$. Along the slow axis, the cylindrical lens behaves like a plane-parallel plate, so the beam (*continuous line*) is essentially unaffected by the lens. (To draw attention to this circumstance, the cylindrical lens is drawn as a dashed line in the figure to indicate that it focuses only on the fast-axis plane.) The beam diameter in the slow-axis plane after the lens is approximately: $D_\parallel \approx L_a + 2f \tan\theta_\parallel$ where L_a is the length of the array. If we now set the condition $D_\parallel = D_\perp$, then we have $f = L_a/2(\tan\theta_\perp - \tan\theta_\parallel)$. Taking $L_a = 200$ μm, $\theta_\perp = 20°$, and $\theta_\parallel = 5°$, we obtain $f = 350$ μm, a focal length that can be obtained with fiber microlenses. With such a small value of focal length, the beam diameter after the lens is $D = D_\parallel = D_\perp = 2f \tan\theta_\perp = 254$ μm which can easily be accepted into, e.g., a 300-μm diameter multimode fiber butt-coupled to the microlens. For a well-corrected fiber microlens, beam divergence after the lens mostly arises from the uncompensated divergence of the slow-axis beam. The fiber NA must then be $NA = \sin\theta_f \geq \sin\theta_\parallel \cong 0.09$. Beam divergence of light leaving the fiber, for a sufficiently long fiber, is then equal to the fiber NA.

In the case of a 1-cm bar, a single, 1-cm-long, cylindrical microlens can be used to focus each array of the bar onto a separate multimode fiber. Since each array is now typically 100 μm long (see Fig. 6.10a), fibers with a 200-μm core diameter and 0.1 NA can be used for each array (see Fig. 6.13). In this way we can convey the whole beam of the bar into 20 fibers whose ends can then be arranged into a circular fiber bundle of 1–1.5 mm diameter, with overall divergence equal to the NA (0.1) of the fiber. The beam emitted by

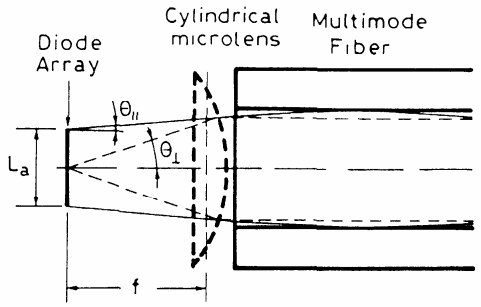

FIG. 6.13. Using a cylindrical microlens to couple the output of a diode array to a multimode optical fiber.

this bundle is then imaged onto the rod along one (Fig. 6.11a) or two longitudinal directions (Figs. 6.11b–c). With this pump configuration, an overall transmission of the transfer system up to 85% has been demonstrated. Output powers up to $\sim$ 15 W in a TEM_{00} mode with an optical-to-optical efficiency of $\sim$ 50% have been obtained, using a Nd:YVO_4 rod pumped by two such fiber-coupled diode bars.

Thermo-Optic Effects

The optical pumping process in a solid-state laser material is associated with the generation of heat for a number of reasons:

(a) The energy difference of the photons between the pump band and the upper laser level is lost as heat to the host lattice; similarly, the energy difference between the lower laser level and the ground state is thermalized. The difference between the pump and laser photon energies, termed quantum defect heating, is the major source of heating in solid-state lasers.

(b) In addition, nonradiative relaxation from the upper laser level to the ground state, owing to concentration quenching, and nonradiative relaxation from the pump band to the ground state will generate heat in the active medium.

(c) In flashlamp-pumped systems, the broad spectral distribution of the pump source causes a certain amount of background absorption by the laser host material, particularly in the ultraviolet and infrared regions of the lamp spectrum. Absorption of lamp radiation by impurity atoms and color centers can further increase heating.

A different way to quantify heat generation is expressed by the parameter χ, defined as the ratio of heat deposited to energy stored in the upper laser level. The theoretical lower limit of η_h for Nd:YAG lasing at 1.06 μm and pumped with a laser diode pump source at 808 nm is $\eta_h = 1 - \lambda p/\lambda L = 0.24$, where $\eta_S = \lambda p/\lambda L$ is the Stokes factor and λp and λL are the wavelengths of the pump and laser beam, respectively.

For example, from the definition of η_h it follows that the ratio of heat to inversion power density available for extraction is $\eta_h/(1 - \eta_h)$. If we account for the resonator losses expressed by the coupling efficiency ηc and for the less than unity overlap of the gain region with the resonator modes expressed by η_B we obtain, for the ratio of heat load to output power,

$$\frac{P_h}{P_{out}} = \frac{\eta_h}{\eta_c \eta_B (1 - \eta_h)}. \qquad \ldots (1)$$

This expression is a lower limit because it does not include the portion of the resonator losses which appear as heat in the active medium as a result of absorption of intracavity laser radiation by the laser material.

Typical examples of heating generated in the laser process are provided in this example. In the laser-diode-pumped systems analyzed in Fig. 6.69 an output of 7 W is associated with 5 W of heating due to the quantum defect and nonradiative processes. This is expressed by $\eta h = 0.32$. In addition, a fraction of the absorption losses also contribute to the heating of the laser crystal. Let us assume that the 7 W output is produced by a 5-cm-long Nd:YAG rod with an absorption coefficient of 10^{-3} cm^{-1}. If the resonator has an output coupler with a reflectivity of 90%, then the intracavity power is 133 W, which produces about 0.7 W of absorption losses in the Nd:YAG rod. Therefore, in the example given in Fig. 6.69, the total heat load for the crystal is around 5.7 W. With this number a ratio of $P_h/P_{out} = 0.81$ is obtained for the laser postulated in Fig. 6.69. In general, one can assume a ratio of

$$P_h/P_{out} = 0.8–1.1 \ldots (2)$$

for a diode-pumped Nd:YAG laser, depending on the crystal quality and the overlap of the resonator and pump region. In flashlamp- or krypton arc lamp-pumped Nd:YAG lasers the thermal load of the crystal is about three times higher

$$P_h/P_{out} = 2.5–3.3 \quad ... (3)$$

The reason for this difference is that the absorbed pump power which is converted into heat depends on whether the upper-state population is extracted by lasing action or depleted by fluorescence. The latter has about a 10% branching ratio into non-radiative decay that contributes to the heat load. Far above threshold, where the upper-state population is extracted by stimulated emission and fluorescence is negligible, thermal loading is decreased.

Temperature Distribution

We consider the case where the heat generated within the laser rod by pump-light absorption is removed by a coolant flowing along the cylindrical rod surface. With the assumption of uniform internal heat generation and cooling along the cylindrical surface of an infinitely long rod, the heat flow is strictly radial, and end effects and the small variation of coolant temperature in the axial direction can be neglected. The radial temperature distribution in a cylindrical rod with the thermal conductivity *K*, in which heat is uniformly generated at a rate *Q* per unit volume, is obtained from the one-dimensional heat conduction equation

$$\frac{d^2T}{dr^2} + \left(\frac{1}{r}\right)\left(\frac{dT}{dr}\right) + \frac{Q}{K} = 0. \qquad \ldots (1)$$

The solution of this differential equation gives the steady-state temperature at any point along a radius of length r .With the boundary condition T (r0) for r = r_0, where T (r_0) is the temperature at the rod surface and r_0 is the radius of the rod, it follows That

$$T(r) = T(r_0) + \left(\frac{Q}{4K}\right)\left(r_0^2 - r^2\right). \qquad \ldots (2)$$

The temperature profile is parabolic, with the highest temperature at the center of the rod. The temperature gradients inside the rod are not a function of the surface temperature T (r_0) of the rod. The heat generated per unit volume can be expressed as

$$Q = \frac{P_{\mathrm{h}}}{\pi r_0^2 l}, \qquad \ldots (3)$$

where *P*h is the total heat dissipated by the rod and *l* is the length of the rod. The temperature difference between the rod surface and the center is

$$T(0) - T(r_0) = \frac{P_{\mathrm{h}}}{4\pi K l}. \qquad \ldots (4)$$

The transfer of heat between the rod and the flowing liquid creates a temperature difference between the rod surface and the coolant. A steady state will be reached when the internal dissipation Ph is equal to the heat removed from the surface by the coolant

$$P_{\mathrm{h}} = 2\pi r_0 l h[T(r_0) - T_{\mathrm{F}}], \qquad \ldots (5)$$

where h is the surface heat transfer coefficient and TF is the coolant temperature. With $A = 2\pi r_0 l$ being the surface area of the rod, it follows that

$$T(r_0) - T_{\mathrm{F}} = \frac{P_{\mathrm{h}}}{Ah}. \qquad \ldots (6)$$

Combining (4) and (6) one obtains, for the temperature at the center of the rod,

$$T(0) = T_{\mathrm{F}} + P_{\mathrm{h}} \left(\frac{1}{4\pi K l} + \frac{1}{Ah} \right). \qquad \ldots (7)$$

Thus, from the geometry, and the appropriate system and material parameters, the thermal profile of the crystal can be determined, except that h must be evaluated.

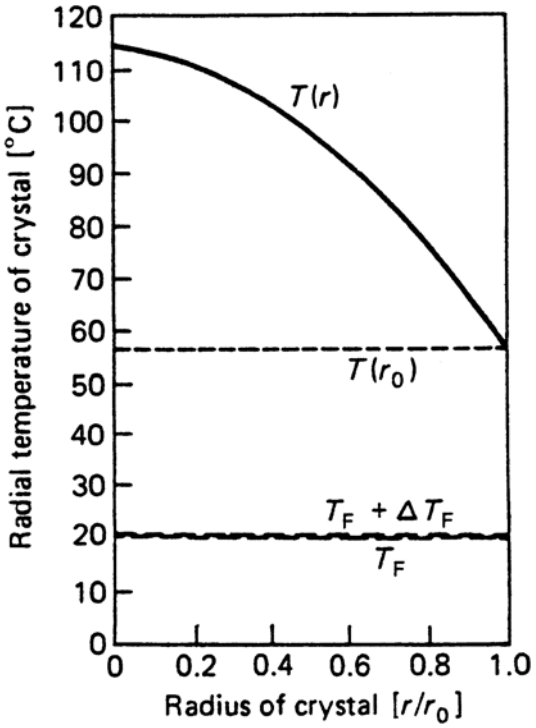

Fig.1. Radial temperature distribution within an Nd:YAG crystal as a function of radius. *T*F is the temperature of coolant entering the flowtube assembly, ΔT_{F} is the axial temperature gradient, and $T(r_0)$ is the rod surface temperature

The convective heat transfer coefficient h is a function of the coolant flow rate, the physical properties of the coolant and laser rod, and the pumping cavity geometry. The boundary conditions for the heat transfer coefficient are a thermally insulated laser rod ($h = 0$) or unrestricted heat flow from the rod surface to a heat sink ($h = \infty$). For cases of practical interest the heat transfer coefficient is typically around $h = 0.5$–2 W cm^{-2} C^{-1}.
If we assume water as the coolant, and a turbulent flow in an annular space formed by a laser rod inside a flow tube, we can greatly simplify the rather cumbersome general expressions for h.

$$h = 10.47 \times 10^{-3} \frac{(D_2/D_1)^{0.53}}{(D_2 - D_1)(D_2 + D_1)^{0.8}} f_r^{0.8} \quad (\mathrm{W/cm\,K}), \qquad \ldots(8)$$

where D_1 and D_2 are the diameter of the rod and the inner diameter of the coolant jacket in cm, respectively, and f_r is the flow rate in cm^3/s. For example, for a rod of diameter $D_1 = 0.3$ cm and an inner diameter $D_2 = 0.8$ cm of the flow tube, we obtain $h = 1.8$ W/cm^2 K for a water flow of 150 cm^3/s.

OPTIMUM OUTPUT COUPLING

For a fixed rate, there is some value for the transmission, T2, of the output mirror that maximizes the output power. Physically, the reason for this optimum arises from the fact that, as T_2 is increased, we have the following two contrasting circumstances: A) The output power tends to increase due to the increased mirror transmission. B) The output power tends to decrease due to the decreased number of cavity photons, ϕ_o, arising from the increased cavity losses.

To find the optimum output-coupling condition, we limit ourselves to a four-level laser and consider the space- independent model. The optimum transmission is then

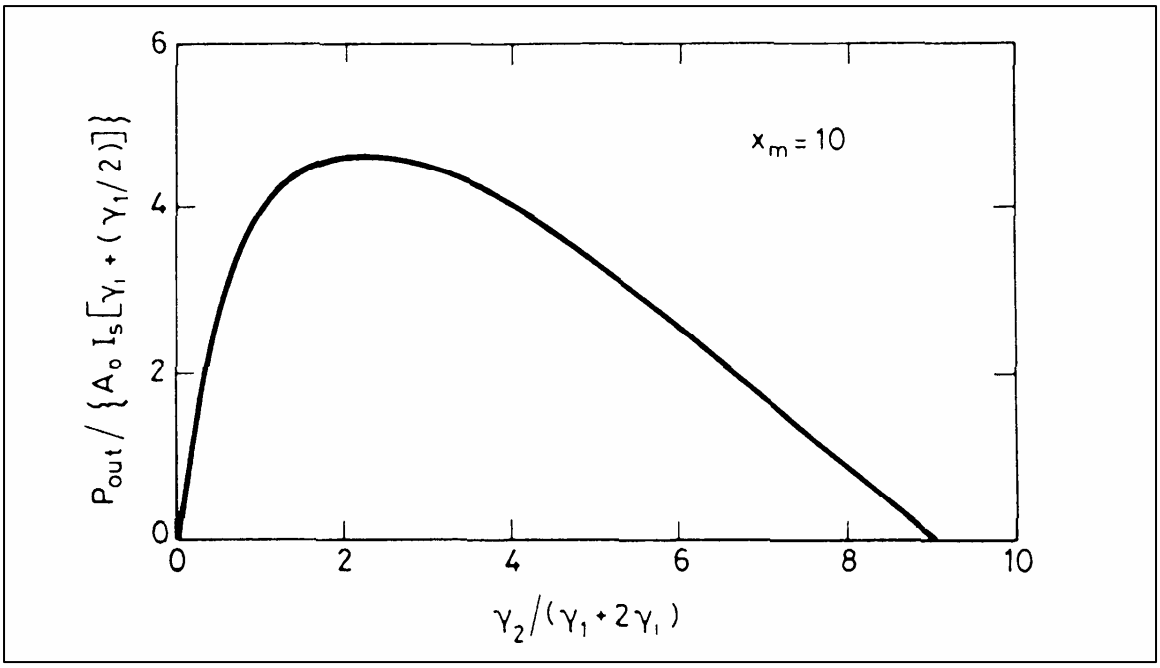

Fig.1. Plot of normalized output power Pout versus normalized transmission of the output mirror γ2 for a pump power, P_p, 10 times larger than the minimum threshold pump power P_{mth}.

Example 7.6. *Optimum output coupling for a lamp-pumped Nd:YAG laser.* We consider the laser configuration discussed in Example 7.2 (see Figs. 7.4 and 7.5) and calculate the optimum transmission of the output mirror when the laser is pumped by a lamp input power of $P_p \simeq 7\,\text{kW}$. Since the threshold power P_{th} in Fig. 7.5 was measured to be 2.2 kW, then according to Eq. (7.5.1) with $\gamma_1 = 0$, we obtain $P_{mth} = P_{th}(\gamma_i/\gamma) \cong 697\,\text{W}$, where the values $\gamma_i \simeq 0.038$ and $\gamma = 0.12$, obtained in Example 7.2, are used for internal loss and the total loss, respectively. We then get $x_m = P_p/P_{mth} \cong 10$, so that from Eq. (7.5.5), $S_{op} \cong 2.17$. From Eq. (7.5.3) we finally obtain $(\gamma_2)_{op} \cong 0.165$, which corresponds to an optimum transmission of $(T_2)_{op} = 1 - \exp[-(\gamma_2)_{op}] \cong 15\%$, i.e., agreeing with the value actually used in Fig. 7.4.